



UNIVERSIDADE TÉCNICA DE LISBOA
INSTITUTO SUPERIOR TÉCNICO

SOLUTE DYNAMICS IN UNSATURATED SOIL

**Trabalho Final de Curso
da Licenciatura em Engenharia do Ambiente**

Pedro Bagulho Galvão
Nº 44786

Orientador: Prof. Ramiro Neves, D^{pto} de Eng.^a Mecânica, IST

Co-Orientador: Eng.º Paulo Chambel Leitão, HIDROMOD

Lisboa, Novembro de 2002

Agradecimentos

A execução deste trabalho de certo não seria possível sem a colaboração de algumas pessoas que de forma desinteressada se mostraram disponíveis para me ceder um pouco do seu conhecimento, às quais devo dizer obrigado

Ao Professor Ramiro Neves, do Departamento de Mecânica do IST, orientador deste trabalho pelos constantes incentivos e boa disposição.

Ao Eng.º Paulo Chambel Leitão, meu co-orientador pela sua dedicação, paciência e empenho no decorrer do trabalho.

Ao Eng.º Pedro Leitão pela orientação prática e constantes sugestões e esclarecimentos.

Por fim de um modo geral a todo o pessoal que actualmente trabalha na Maretec, todos contribuíram para este trabalho ao proporcionarem um óptimo ambiente de trabalho.

Não podia deixar de agradecer aos meus pais e irmão que me apoiaram ao longo de toda uma etapa que atinge o final com este trabalho.

Summary.

Nitrogen contamination of ground and surface waters is a major environmental problem that is recognized in the nitrate directive of the European union.

This and many other problems have been addressed by IST's group of marine research –MARETEC. Over the last few years, this research group has developed the MOHID system, a numerical tool that simulates water flow and quality for estuaries, lagoons and open sea. Soil water flow and solute transport routines have been introduced over the last few years in MOHID, so Nutrient cycle processes are the next logical step.

This work tries to add to MOHID the capacity to model the water quality while it's still in the agricultural soils, one of the major sources of nitrate pollution. This can be faced as the first steps in a long road that may lead to a fully integrated water flow and quality toll.

Nitrogen cycle in soil is the sum of bacterial driven processes. This "driving force", like any other living organism, needs a delicate nutrient balance. Since in soil carbon is usually the limiting nutrient, and integrated approach on both cycles is needed.

An initial approach to modeling these cycles was done trough the use of the POWERSIM software package. This resulted in an initial zero-dimensional model. Later this initial model was coded in FORTRAN, and implemented in a new module in MOHID, gaining three-dimensional functionality.

Test runs where produced with realistic values, simulating several situations of terrain morphology and irrigation practices.

Keywords: Soil water flow, Solute transport, Nitrogen cycling, Carbon cycling, nitrate leaching

INDEX

CHAPTER 1.....	1
1.1- INTRODUCTION	1
1.2- BASIC CONCEPTS	3
1.2.1- <i>Mineralization</i>	5
1.2.2- <i>Immobilization</i>	5
1.2.3- <i>Nitrification</i>	6
1.2.4- <i>Denitrification</i>	7
1.3- RESUME	8
1.4- WORK GUIDELINES	9
CHAPTER 2.....	10
2.1- CYCLE MODELING.....	10
2.2- EXISTING MODELS (STATE OF THE ART).....	12
2.3- POWERSIM, AN INITIAL MODEL	14
2.3.1- <i>Model conceptualization</i>	15
2.3.2- <i>Carbon Pools</i>	17
2.3.3- <i>Nitrogen Pools</i>	18
2.3.4- <i>Autotrophic processes</i>	19
2.3.5- <i>Heterotrophic processes</i>	20
2.3.6- <i>Anaerobic processes</i>	23
2.3.7- <i>Global balance</i>	25
2.4- POWERSIM ANALYSIS.....	26
2.5- FORTRAN IMPLEMENTATION.....	29
2.5.1- <i>System Solution</i>	31
2.5.2- <i>General Module Structure</i>	32
2.5.3- <i>Initial Results Analysis</i>	33
CHAPTER 3.....	35
3.1- SIMPLE SOIL COLUMN	35
3.2- WHY GO DOWNHILL?.....	40
3.3- DON'T BE DEPRESSED	43
3.4- COVER IT UP	44
CHAPTER 4.....	45
4.1- CONCLUSION / FUTURE WORK	45

REFERENCES

Appendix I : Soil Water flow

Appendix II : Solute transport in unsaturated soil

Appendix III : Alvalade Data

Appendix IV : Macro programming

Appendix V : Brief MOHID history

CHAPTER

1

1.1- Introduction

Modern agriculture relies on irrigation systems supported by the use of chemical products and fertilizers. These modern practices have the advantage of increasing productions but if mislead, can cause serious environmental and economical harm.

Nitrogen is usually the most utilized compound in agricultural fertilization. It is an essential nutrient for amino acids and some Vitamin synthesis (Vos, 1994 as in Cameira, 1999). Because of its nutritional importance and relative scarcity, protein is highly sought by most animals, humans included.

More money and effort have been, and are being spent on the management of Nitrogen than any other mineral element. According to Brady, 2002 the worlds ecosystems are probably more influenced by deficits and excesses of Nitrogen than any other mineral element.

On one hand, the pale yellowish green foliage of nitrogen-starved crops forebodes crop failure, financial ruin and hunger for people in all corners of the world. On the other excesses of some nitrogen compounds in soil can adversely affect human and animal health and denigrate the quality of the environment.

High nitrogen levels in soil can lead to sufficient high nitrates in drinking water as to endanger the health of human infants and ruminant animals. For that reason, nitrate levels are monitored in wells, reservoirs, and other drinking supplies. The movement of soluble nitrogen compounds from soils to aquatic systems can disrupt the balance of those systems, leading to eutrophication, decline in oxygen content, and the subsequent death of fish and other aquatic species. Supplying sufficient nitrogen often represents a major expense in agricultural production. In addition, the manufacture of nitrogen fertilizer accounts for a large part of the fossil fuel energy used by the agricultural sector.

However, according to Brady 2002, even in regions with high leaching potential, careful up soil management can prevent excessive nitrate losses. The timing of modest fertilizer and manure applications should provide Nitrogen when the plant needs it, not much before or after the period of active plant uptake. If this is not economically possible, other crops in the rotations, such as cover crops, should be planted immediately following the cash crop to take the unused nitrates.

The same author claims that if good nitrogen management practices are followed, nitrogen leaching may be kept to less than 5 or 10% of the applied Nitrogen

At a European level, two documents address this problem. Directive COM 80/788 establishes a maximum, um value of NO_3^- at 50 mg l⁻¹ for drinking water. The Nitrate directive (91/676) also acknowledges the excessive use of fertilizers as an environmental risk. Sensible areas, where agricultural practices should be restrained in the moment and quantity of applied fertilizations, are defined. These sensible zones are defined as those that drain, directly or indirectly, to superficial or underground waters that are used as drinking water sources, or those that drain to lakes, fresh water, estuaries, costal waters or oceans that show eutrophication events. However, no indications are supplied on which procedures should be adopted leaving this up to good management practice principles.

In Portugal, recent studies indicate an increase of nitrate in superficial and underground waters because of the increasing application rates of nitrogen fertilizers (Follet 1989 as in Cameira 1999).

According to Cameira 1999, no data is available to quantify this problem, even though vulnerable zones have been established in Ribatejo, Campina de Faro and Vale do Vouga, where NO_3^- concentration in underground waters surpass the maximum admissible value for human consumption.

For all this, in a sustainable agriculture, mineral Nitrogen should be considered an essential element, subject of careful application planning. However, this application planning is not simple, difficulties arise due to the great variety of processes that must be understood.

When faced with the variety and complexity of these processes (ex: soil water movement, biochemical transformation processes) that influence Nitrogen dynamics in soil, computational models can be considered a fundamental tool for a sustainable agriculture.

Over the last three decades, efforts where placed on the development of mathematical models that can be used to predict the transport of solutes in unsaturated soil.

These models embrace several disciplines and in most of the cases are extremely complex and oriented to a specific application (see *2.2-Existing models (state of the art)*).

An extensive application of these types of models to Portuguese soils is the work of Cameira, 1999 where RZWQM model (Root Zone Water Quality Model) was calibrated and applied to controlled agricultural soils.

MARETEC, marine modeling group of IST, is also alert to this problem. Over the last few years, routines that predict water flow and mass transport in unsaturated soil have been introduced in MOHID (Neves (2000) et al. and Neves et al. (2002)).

Even though MOHID was initially developed to simulate bi-dimensional water flow in costal areas (Neves, 1985), its sphere of action has been successively enlarged to Boussinesq Waves (Silva, 1992), water quality (Portela, 1996), and three-dimensional water flows (Santos, 1995; Martins 2000).

With the inclusion of soil water quality routines, steps are taken to an integrated model where water flow and quality can be simulated from the moment it infiltrates the soil to the ocean.

Applications of MOHID to Portuguese soils can already be found in Neves *et al.* 2002, where water flow was simulated and Chambel Leitão *et al.* 2003, where soil water flow and Sodium transport were simulated for a bear soil in Alvalade.

For all this, this work aims the development of soil water quality routines that can predict Nitrogen dynamics in soil water, and integrate these routines with the available mass transport routines of MOHID, creating a three-dimensional soil water quality model.

1.2- Basic Concepts

Some 75,000 Mg of nitrogen is found on the air above one hectare of soil (Brady 2002). The atmosphere, which is 78% gaseous nitrogen, appears to be a virtually limitless reservoir of this element. However, the very strong triple bond between two nitrogen atoms makes this gas quite inert and not directly usable by plants or animals. The nitrogen content of a surface of mineral soils normally ranges from 0.02 to 0.5%. A hectare of such a soil would contain 3.5 Mg nitrogen in the A horizon and an additional 3.5 Mg in the deeper layers. While these figures are low compared to those of the atmosphere, the soil contains 10 to 20 times as does the standing vegetation.

The soil, nitrogen fraction undergoes a series of complex biochemical transformations. These processes have long been the subject of intense scientific investigation. Along with some atmospheric Nitrogen transformations, these processes are grouped in the Nitrogen cycle.

As a Nitrogen atom moves through the cycle, it may appear in many different forms, each with its own properties, behaviors and consequences for the ecosystem. Understanding these transformations is the key to solve the environmental, agricultural and natural resource problems stated in the previous chapter.

This cycle also explains why vegetation, and indirectly animals can continue to remove nitrogen from the soil for centuries without depleting the soil from this essential nutrient. The biosphere does not run out of nitrogen because it uses the same nitrogen repeatedly.

The principle pools and form of nitrogen, and the process by which they interact in the cycle are illustrated in *Figure 1.1- Nitrogen Cycle* (adapted from Brady 2002).

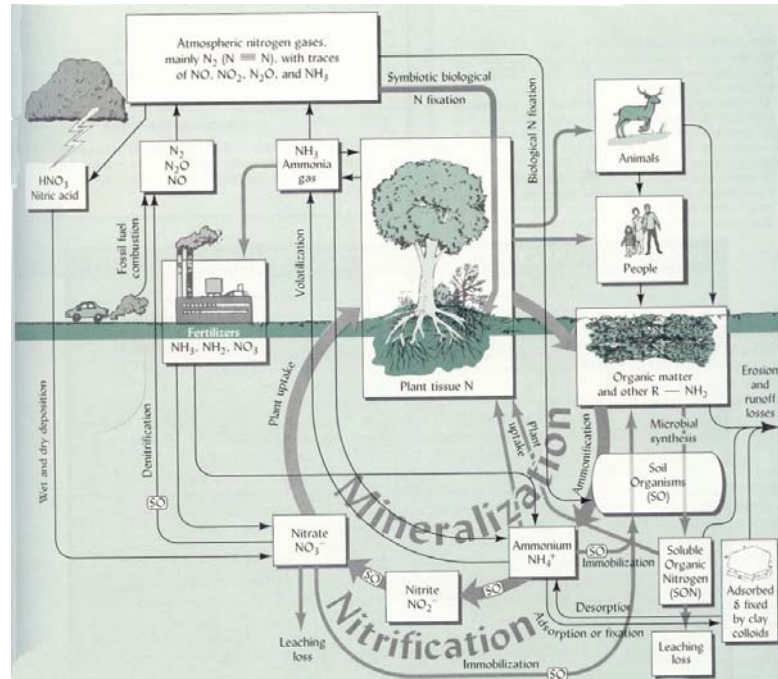


Figure 1.1- Nitrogen Cycle

The primary cycle is emphasized with heavy, dark arrows. In a general description, organic nitrogen is mineralized, plants take up the mineral nitrogen, and eventually organic nitrogen is returned to the soil as plant residues. Note also that through some pathways nitrogen is lost from the soil (leaching, runoff, denitrification and volatilization). These loss processes mainly affect the more mobile forms of Nitrogen, the mineral forms, Ammonia NH_4^+ and Nitrate NO_3^- . However, leaching only affects the NO_3^- form of nitrogen in a significant manner. This happens because like other positively charged ions, ammonium ions are attracted to the negatively charged surfaces of clay and humus, where they are partially protected from leaching. On the other hand Nitrate particles do not form insoluble compounds with the usual soil solution constituents, nor is retained in its colloidal complex due to its negative charge (Santos, 1980 as in Cameira, 1999).

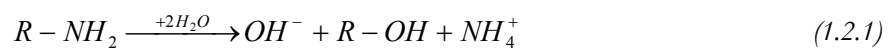
Soil organisms are the driving force for most of the reactions in the cycle (Brady 2002). They are represented by boxes with rounded ends (labeled "SO") in the diagram. They create enzymes that catalyze the different biochemical reactions, either in their microbial bodies or in adjacent sites where the enzymes may have been excreted. Truly, the Nitrogen cycle is dominated by microbial action (Alexander, 1961).

The next sections try to resume the theoretical basis of each of the primary cycle processes.

1.2.1- Mineralization

The great bulk of soil nitrogen is in organic compounds that protect it from loss, but leave it largely unavailable to higher plants (Brady 2002). Much of this nitrogen is present as amine groups ($R-NH_2$) in proteins or as part of humic compounds.

When soil microbes attack these compounds, the long chains of amino acids are broken and individual amino acids appear in the soil solution along with dissolved CO_2 . Then the amine groups are hydrolyzed, and the nitrogen is released as ammonium ions (NH_4^+). This enzymatic process is termed **mineralization**. (1.2.1) is an example of an amino compound acting as a mineral nitrogen source.



Mineralization happens when Heterotrophic microorganism attack the carbonaceous materials both in order to obtain energy and construction materials for their cells. However, no organisms can prosper on carbon alone. Nitrogen is also an essential building block of cells structure. Part of the obtained Nitrogen is used for new cells construction and part is lost in the form of the ammonium ion.

At this point the intimate relations between the Carbon and nitrogen cycle become apparent. Carbon is the major building block of any life form, including the soils microorganisms that thrust the Nitrogen transformations on soil. This relation further narrows since Nitrogen it self is also a vital element for the same microorganisms (1.2.2-Immobilization)

According to Brady et al. 2002, many studies indicate that only about 1.5 to 3.5% of the organic nitrogen of the soil mineralizes annually. Even so, this rate of mineralization provides sufficient mineral nitrogen for normal growth of natural vegetation in most soils. Exception is made to those soils with low organic matter content, such as soils of deserts and sandy areas. The same author claims that isotope tracer studies on farmlands that have been emended with synthetic nitrogen fertilizers show that mineralized nitrogen constitutes a major part of nitrogen taken up by plant. If the organic matter content of soil is known, one can make a rough estimate on the amount of nitrogen likely to be released by mineralization.

1.2.2- Immobilization

The opposite of mineralization is immobilization, the conversion of organic Nitrogen ions to organic forms. Immobilization can take place by both biological and non-biological processes (Brady et al. 2002). In the biological processes, as microorganisms decompose the carbonaceous organic residues, they use part of these residues as building material and part as cell "fuel", oxidizing carbon to produce energy.

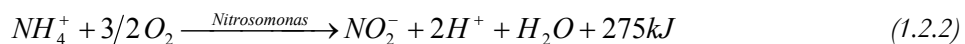
However, the Carbon / Nitrogen composition of most living being must be kept under a constant ratio. If sufficient Nitrogen is not found in the decomposed residues themselves, the microorganisms have the

capacity to incorporate mineral nitrogen ions into their cells proteins, balancing the lack of organic Nitrogen. This can deplete the soil solution of mineral forms of Nitrogen. When the organisms die, some of the organic nitrogen in their cells converts into forms that make up the humus complex, and some may be released as ammonia.

Mineralization and immobilization occur simultaneously in the soil (Brady et al. 2002), whether the net effect is an increase or a decrease in the mineral nitrogen depend essentially on the ratio of carbon to nitrogen in the residues undergoing decomposition.

1.2.3- Nitrification

Certain soil bacteria may enzymatically oxidize ammonium ions in the soil, yielding first nitrites and then nitrates. These bacteria are classified as Autotrophs, even though a more correct term would be Chemoautotroph, because they obtain their energy from oxidizing the ammonium ions rather than organic matter. The process termed nitrification consists of two main sequential steps. The first step results in the conversion of ammonium to nitrite, by a specific group of autotrophic bacteria (*Nitrosomonas*). The nitrite so formed is immediately acted upon by a second group of Autotrophs, *Nitrobacter* (Alexander, 1961). The enzymatic oxidation releases energy and may be represented as:



So long as conditions are favorable for both reactions, the second transformation follows the first closely, preventing the accumulation of nitrite. According to (Brady et al. 2002) this is fortunate since even at low concentrations (just a few part per million), nitrite is quite toxic to most plants and mammals.

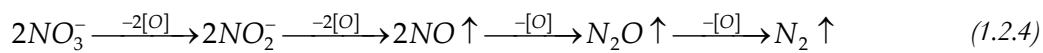
During the nitrification process, part of the nitrogen contained in the ammonium ion, is retained by the autotrophic biomass and is used to form new cells. Again, microbial CN¹ ratio must be kept within strict limit. In these cases CO₂ is immobilized by the autotrophic biomass.

Regardless of the source of ammonium (fertilizer, sewage, animal manure, etc) nitrification will increase soil acidity by producing H⁺ ions.

¹ Carbon / Nitrogen

1.2.4- Denitrification

Nitrogen may be lost to the atmosphere when nitrate ions are converted to gaseous forms of nitrogen by a series of widely occurring biochemical reductions termed **denitrification**. The organisms that carry out this process are commonly present in large numbers and are mostly facultative anaerobic bacteria in genera such as *Pseudomonas*, *Bacillus*, *Micrococcus*, and *Achromobacter* (Brady et al. 2002). These organisms are Heterotrophs, and as so obtain their energy from the oxidation of organic compounds. However, instead of using oxygen as an electron receiver, Nitrate is used oxidant for the organic carbon. Nitrate, $NO_3^- [N(V)]$ is reduced in a series of steps to nitrite $NO_2^- [N(III)]$, and then to Nitrogen gas that include $NO [N(II)]$, $N_2O [N(I)]$ and eventually $N_2 [N(0)]$



Although not shown in the simplified reaction given here, the oxygen released in each step would be used to form CO_2 from organic Carbon.

For these reactions to take place, sources of organic residues should be available to provide the energy the denitrifiers need.

Since Oxygen is a much stronger oxidant than Nitrate, the denitrification process gains importance when the air in the soil's microsites becomes limiting (usually less than 10%) (Alexander, 1961).

Generally, when oxygen levels are low, the end product released from the overall denitrification process is Dinitrogen gas (Brady et al. 2002). However it should be noted that $NO [N(II)]$ and $N_2O [N(I)]$ are commonly also released during normal denitrification, that suffer from the fluctuation aeration conditions that often occur in the field.

The question of how much of each nitrogen gas is produced is no merely of academic interest. Dinitrogen gas is inert and environmentally harmless, but nitrogen oxides are very reactive gases and can cause environmental damage in at least four ways:

- Contribute to the formation of nitric acid (component of acid rain)
- Formation of ground level ozone
- Greenhouse effect (if it reaches the higher atmosphere)
- Destruction of ozone (if it reaches the higher atmosphere)

If nitrate supplies are very low, denitrification processes cannot function, but certain methanogenic bacteria use alternative oxidants and produce methane gas.

1.3- Resume

In global view, nitrogen cycling in soil is a complex process controlled by soil's microorganisms. These microorganisms, such as any living being need to balance their nutrient uptake and, if the situation arises, mineral forms of nitrogen can be used to balance the lack of Organic Nitrogen. This situation can drain the soil of mineral forms of nitrogen during long periods, causing higher plants to suffer from nitrogen deficiency, but at the same time avoiding Nitrogen leaching, see *Figure 1.2- Nitrate depression period*.

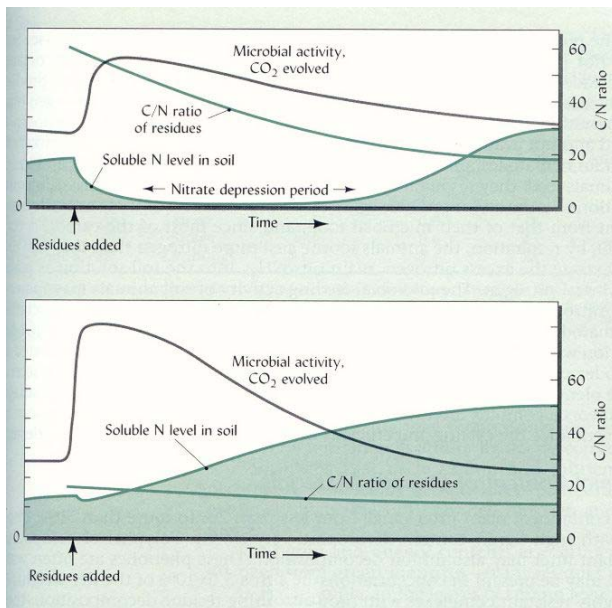


Figure 1.2- Nitrate depression period

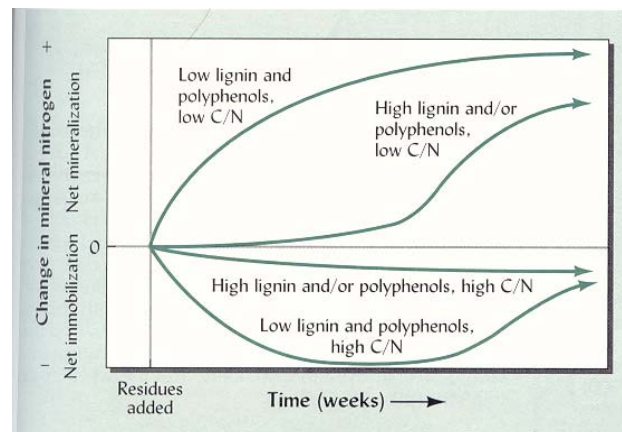


Figure 1.3- Residue quality influence on the depression period

If the applied residues, have a high CN ratio, nitrogen depression periods are likely to appear, but the residue quality also affects the rate of net mineralization. Residues high in phenol and lignin (large and complex structures difficult to degrade) can have narrow CN ratios, but due to the slow decomposition process, release nitrogen quite slowly – often too slow to keep up with the needs of the growing crop (Brady et al. 2002) *Figure 1.3- Residue quality influence on the depression period*

Ammonium ions are not leached easily, due to the attraction to the positively charged surfaces of the negatively charged surfaces of clay and humus. However, even though the adsorbed ammonium ions are exchangeable for most soils microorganisms, they become out of reach for higher plants.

As so in good nitrogen management practices all these factors should be conjugated to produce nitrate as plants need it, avoiding nitrogen leaching and maximizing plant used nitrogen.

Adding to the previous, important theoretical basis for this modeling work are the soil water flow and transport equations. Explanations of the theoretical biases and the MOHID implementation of such principles can be found in *APPENDIX I and II*.

1.4- Work guidelines

A three-dimensional model for soil water quality faces several difficulties, such as large spatial gradients, interactions with soil chemistry and biology, etc. As so, the soil water quality routine that will be developed during this work must be as flexible as possible. In addition, MOHID code is constantly growing, spaces for future interactions should also be predicted.

Having this in mind, a global overview of existing models lead to the selection of a particular type of specific rates calculations used by a very complete and agricultural oriented model named RZWQM, Chapter 1.1 further explains this selection.

One of the major the major differences between existing models is the way carbon and nitrogen pools should be divided, and how they interact among them.

An attempt was made to leave these interactions as generic as possible, leading to a labile and a refractory Carbon pools. The Carbon / Nitrogen of the labile pool is allowed to vary freely during the simulations. Limiting factors for microbial action are one of the main innovations proposed in this study. The way these limiting factor are calculated is original.

Another interesting question that may be answered from this work is that of the importance of three-dimensional models for soil water flow and quality. Usual these type of models are either uni or bi-dimensional.

This work is divided into chapter. A general description follows.

Chapter II

In the first part of this chapter, the different existing models for soil water quality are analyzed.

Next, a conceptual model is built and the used process rate equations are described. An implementation of this model is done using the POWERSIM software package.

In the third part, the zero dimensional model is passed into FORTRAN code. How this code is implemented in MOHID is explained in this chapter.

Chapter III

Test runs are made with the newly created three-dimensional water quality model, and results are analyzed.

Chapter IV

Conclusions are taken and future directions are pointed.

2.1- Cycle modeling

The previous chapter introduced the complex processes that affect Nitrogen in soil. Several chemical species interact with soil biodiversity and create sinks and sources for Nitrogen. Soil water can lead to anaerobic conditions, affecting the microorganisms responsible for the biochemical processes, or it can transport one or several of the cycle components.

This work aims to model these biochemical processes in MOHID. A brief introduction to MOHID can be found in APPENDIX V.

As said before several properties including nitrate are transported by water, so the first step for nitrogen cycle modeling must be the correct prediction of water fluxes in soil, since the leached nitrate is the major environmental problem and aim of this work. The unit flux per total soil area \vec{J}_w can be predicted by *Darcy-Buckingham* flux law

$$\vec{J}_w = -K(h)\nabla H \quad (2.1.1)$$

A full introduction to water flow in unsaturated soil and the way it was implemented in MOHID can be found in *APPENDIX I*.

Once the water fluxes are correctly evaluated, the first law of thermodynamics will lead to the advection - diffusion equation for soil properties. In an Eulerian referential:

$$\frac{\partial \theta c}{\partial t} + \frac{\partial \rho s}{\partial t} = \nabla \cdot [\theta D_2^w \nabla (c_2) - \vec{J}_w c_2] - (\mu_{w,2} + \mu'_{w,2}) \rho s_2 - S_{c_{r,1}} - (\mu_{w,1} + \mu'_{w,1}) \theta c_1 \quad (2.1.2)$$

The full derivation and MOHID implementation of dissolved properties evolution is explained in *APPENDIX II*.

Equation (2.1.2) results from a full mass balance on a given property. It is the result of water transport process, partition processes and biochemical processes.

MOHID follows a numerical method termed “*approximate factorization*” (Fletcher, 1997 as in Leitão 2002). In a general manner, this method solves each of the different terms of equation (2.1.2) separately and adds them to obtain the new property concentration. An initial “approximation” of the new property concentration is made by solving, for instance, the transport part of (2.1.2). To this new approximated value, the partition

processes are added, and then the biochemical processes, and so on. No time splitting occurs for any of these approximations, so all the processes are solved independently for each time interval.

$$\begin{aligned}
 P^1 &= f(P^t, P^1, \dots) & \wedge 1 &\rightarrow \text{Advection/ Difusion} \\
 P^2 &= f(P^1, P^2, \dots) & \wedge 2 &\rightarrow \text{Partition Processes} \\
 P^3 &= f(P^2, P^3, \dots) & \wedge 3 &\rightarrow \text{Biochemical cycling}
 \end{aligned}$$

Figure 2.1 - Property evolution

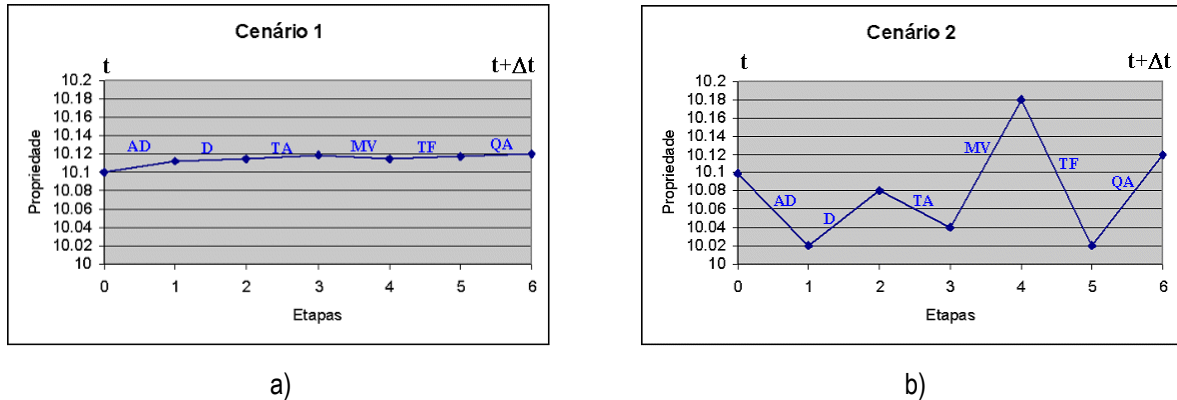


Figure 2.2- Imaginary scenarios for the effects of different processes (represented by AD, D, TA, MV....)
adpated from Leitão 2002

A disadvantage that may arise from this iterative method, is that if the module of the total variation is smaller than the module of the variations that occur in each of the “approximations” (Figure 2.2 – (a) as in opposite to (b) where the module of every approximation is smaller that the total variation), this method may not display good results. However, according to Leitão, 2002 this numerical method as shown good stability in diverse MOHID applications (ex: Ocean, estuaries).

The main advantages of such an approach are the different space and time discretization for each of a property evolution terms. Also new processes such as (in this case) the nitrogen cycle can be added without major changes to the existing program’s code.

Adding to this MOHID uses an object oriented approach (Miranda et al. 2000), which isolates the parts of the code that model the different processes, allowing full control on how these different parts interact and

An initial zero-dimensional model was created to simulate the integrated Carbon / Nitrogen cycle, using the POWERSIM software package. This initial model was then reprogrammed in FORTRAN and implemented into a new module in MOHID, gaining access to the already available soil water flow and mass transport routines. The result was a three-dimensional model for soil Carbon / Nitrogen cycle.

The next chapters will introduce the way these models (POWERSIM and SEDIMENTQUALITY) were developed.

2.2- Existing models (state of the art)

Over the past decades, several attempts have been made to predict the fate of Nitrogen in soil, resulting in different degrees of detail and different application scales. Examples of such diversity can be found in Shaffer 1995, models such as **EPIC**, Williams et al. 1948; **GLEAMS**, Knisel (1993); **NLEAP**, Shaffer et al. (1991); **NTRM**, Shaffer and Larson (1987); **LEACHM-N**, Wagemet and Hutson (1989); **CENTURY**, Wetherell et al. (1993); and **RZWQM**, USDA (ARS (1992)). These models predict nitrate leaching below the root zone and some like **RZWQM** account for different soil management practices and cultures. However, they are all one-dimensional models.

Other models such as **HYDRUS** have a more physical approach and present a two-dimensional water flow calculus. However, no element cycles are available. Simplified simulations are obtained by adding sink and source terms to the advection diffusion presented in (2.1.2). The terms impose a constant transfer rate between properties.

According to Neves et al. 2000 **HYDRUS** enjoys large acceptance in the scientific community, due to the large amount of publications that supports the software. Since **HYDRUS** was used to calibrate soil water flow in MOHID, more information about it can be found in *APPENDIX I*.

Nitrogen transformations modeling in Europe, according to Hansen et al. 1995, has had the tendency toward using more simple kinetics in the turnover of organic matter in soil. On the other hand in the United States, emphasis has been placed on the unification of N-cycle equations and the development of simplified N models suitable for use by action agencies and agricultural producers.

The same author divides modeling approaches used in the simulation of net nitrogen mineralization into three categories:

- Models, which do not consider carbon decomposition and characterize the soil organic matter only on its nitrogen content.
- Models which characterize the soil organic matter in terms of its carbon and nitrogen content but, do not consider microbial biomass explicitly.
- Models that characterize soil organic matter in terms of carbon and nitrogen and consider microbial biomass explicitly.

Models of category 1 have, in general, the advantage of being simple but the range of condition where they are applicable is limited, because carbon is usually the nutrient limiting the Nitrogen cycle turnover rate. Models of categories 2 and 3 require simulation of both the carbon and nitrogen cycles, which leads to additional computation time, but gain flexibility. Finally models of type 3 have the advantage of explicitly simulating the variation of the cycle properties transformation rates with the available microbial biomass and environmental processes that affect them, but need more field data.

In models which consider biomass explicitly, usually the Monod kinetics model (2.2.1) is used to predict the specific decay or growth rates

$$\frac{\partial S}{\partial t} = \mu_m \frac{S}{K_s + S} B \quad (2.2.1)$$

Where S is the substrate (carbon concentration), B is the size of the microbial pool, μ_m is the maximum specific growth rate and K_s is the half saturation constant.

Sometimes first-order reaction kinetics (2.2.2) and zero-order kinetics (2.2.3) are also used.

$$\frac{\partial S}{\partial t} = K_1 S \quad (2.2.2)$$

$$\frac{\partial S}{\partial t} = K_0 \quad (2.2.3)$$

First and zero order kinetics consider that microorganisms have an unlimited potential for decomposing organic substrate, nitrify, denitrify, etc. or that this maximum transformation rate is never reached, due to substrate limitation. The zero order kinetics approach also assumes that these transformations are independent of the substrate concentration.

According to Hansen et al. 1995, neither of these assumptions is generally true, but may prove to be good approximations over a determined range of conditions. It is very important to remember that these expressions are empirical and that expressions for specific growth and decay rates (represented by K_1 in (2.2.2)) have been proposed by a number of authors (Monod, Teissier, Contois and Moser).

Metcalf and Eddy, 1991 states that what is fundamental in the use of any rate expression is its application in a mass-balance analysis, and not, its relation to those commonly presented in the literature. The same author claims that it is equally important to remember that specific rate expressions should not be generalized to cover a broad range of situations based on limited data or experience.

As far as environmental factors that affect nitrogen dynamics in soil, temperature and moisture content are considered, according Hansen et al. 1995, the most important environmental factors affecting the microbial action. The effect of temperature is usually expressed according to an Arrhenius-type equation (2.2.4),

$$e_t = A \exp(E/T) \quad (2.2.4)$$

Where T is the temperature, E and A are empirical coefficients.

Soil moisture affects the microbial action reducing the oxygen supply, and other factors such as salinity. In most models, according to Hansen et al. 1995, the effect of soil moisture on decomposition rates is expressed by empirical function.

Another common factor in these models is the division of substrates into different pools, each with different decay rates. This division usually changes from author to author and can be regarded as a major problem in mineralization models. This fractioning is to some degree arbitrary, as so decomposition kinetics are in many cases model specific, and end up depending on the model objectives.

In RZWQM, USDA (ARS (1992), numerical model an attempt was made to unify the form of the process rate equations governing carbon and nitrogen cycling in soil and provide a firm theoretical basis for environmental interactions (Shaffer et al. 1999). The basic form of the specific decay rate this model uses is (2.2.5)

$$K = f_{aer} \left(\frac{k_b T_f}{h_p} A_i \right) \exp \left(- \frac{E_a}{R_s T_t} \right) \frac{[O_2]}{[\gamma_1 H]^{K_H}} Pop \quad (2.2.5)$$

In this model (RZWQM), all of the cycle processes, including microbial growth and death, are modeled by first order reaction kinetics, with the specific rate defined by a similar equation to (2.2.5). Further analysis on these equations and equation (2.2.5) can be found on the next sections.

The RZWQM model has been developed over the past ten years and besides the Nitrogen / Carbon cycle, simulated in the OMNI sub model, it also models the growth of the plant, the movement of water and agrochemicals, within and below the crop root zone of an agricultural cropping system under a range of common management practices.

This model has been applied to Portuguese soils in the work of Cameira 1999, and as so makes an interesting starting point for the development of soil Carbon / Nitrogen cycle in MOHID.

2.3- POWERSIM, an initial model

At this point precious help came from the use of POWERSIM. This software package was initially developed for business simulation, but it can be of great assistance in environmental modeling since it allows to visually build a zero-dimensional model. Conceptual errors can be eliminated in an early stage, never reaching the “real program” code.

POWERSIM allows several time discretization such as the explicit or Euler method up to the, fourth order Runge Kuta method, with variable time step.

The next section explains how this “visual” model was created.

2.3.1- Model conceptualization

The MOHID soil Carbon / Nitrogen cycle module should simulate microbial biomass explicitly, in order to respond to physical changes of the soil, such as variation of water contents, temperature, etc.

This model will use transitional state rate equations, Laidler (1969), Shaffer and Dutt (1974); Shaffer (1985), present in Shaffer et al (1998). These equations include Arrhenius temperature response functions, reactive constituent concentrations, and simulate responses to soil oxygen levels, pH, water content and salinity.

Element properties will be modeled by first order kinetics following the RZWQM specific rates formulation (2.2.5). For example for Nitrification:

$$K_{nitrification} = f_{aer} \left(\frac{k_b T_{nitrification}}{h_p} A_{nitrification} \right) \exp \left(- \frac{E_a}{R_g T_{nitrification}} \right) \frac{[O_2]^{0.5}}{[\gamma_1 H]^{k_H}} Pop_{Autotrophs} \quad (2.3.1)$$

Where $K_{nitrification}$ is the first order nitrification rate [day^{-1}] and:

f_{aer} - Empirical adimensional parameter

$T_{nitrification}$ - Nitrification temperature [$^{\circ}K$]

K_b - Boltzman constant $1.383E-23$ [$J^{\circ}K^{-1}$]

h_p - Planck constant $6.63E-34$ [$J s$]

$A_{nitrification}$ - Nitrification rate coefficient [$s day^{-1} pop^{-1}$]

E_a - Activation energy [$kcal mole^{-1}$]

R_g - Universal gas constant $1.99E-3$ [$kcal mole^{-1}^{\circ}K^{-1}$]

$[O_2]$ - Oxygen concentration in soil water assuming that soil air O_2 not limited [$moles O_2 m_{water}^{-3}$]

$[H]$ - Hydrogen ion concentration [$moles H m_{water}^{-3}$]

γ - Activity coefficient for monovalent ion

k_H - Hydrogen ion exponent for nitrification

$Pop_{autotrophs}$ - Population of autotrophic microbes [$\# organisms kg soil^{-1}$]

Anaerobic effects are expressed by f_{aer} that varies from 1 to 0 according to the effective soil water content θ_{ef} . $[O_2]$ is the maximum available dissolved oxygen (in saturation conditions). The rate is affected by Oxygen limitations thru the use of f_{aer} see chapter 2.5.2-*General Module Structure*.

The activation energy, E_a , is the sum of a constant apparent activation energy with the ionic strength times a salinity coefficient. The salinity coefficient and the apparent activation energy are pool specific. This formulation produces an exponential variation with the ionic strength, but will not be implemented in this initial model due to lack of available data. Instead, a medium value for the apparent activation energy is used.

Microbial populations enter explicitly in the specific rate (in the case of nitrification the autotrophic population is present). RZWQM presents relations between Carbon concentrations and effective populations for every microbial pool.

The nitrification temperature is equal to the soil temperature when it does not exceed a certain maximum temperature of nitrification. If the soils temperature exceeds this value, the nitrification temperature will follow (2.3.2), and the specific rate (2.3.1) will vary according to *Figure 2.3*

$$T_{nitrification} = 2T_{max} - \text{soil temperature} \quad (2.3.2)$$

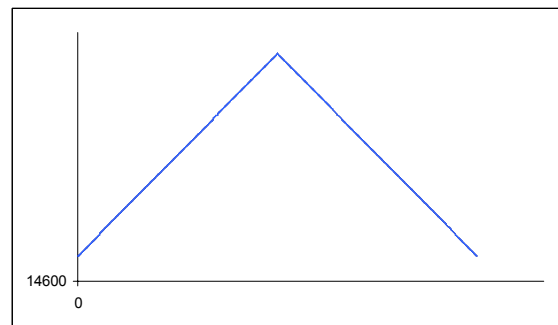


Figure 2.3- Specific rate coefficient variations with Temperature

For biomass death a similar equation to (2.3.4) is used

$$K_{nitrification} = f_{aer} \left(\frac{k_b T_{nitrification}}{h_p} A_{nitrification} \right) \exp \left(- \frac{E_a}{R_g T_{nitrification}} \right) \frac{[O_2]^{0.5}}{[\gamma_1 H]^{k_H}} Pop_{Autotrophs} \quad (2.3.3)$$

Again all the coefficients are specific for each microbial pool.

Some environmental effects like anaerobiosis, pH, etc are considered in both the microbial growth and decay. For instance lack of oxygen (expressed by f_{aer}) can stop aerobic organic matter decay or Ammonia nitrification (according to (2.3.1)), but at the same time it will also increase the mortality rate of all aerobic pools. This accounts for both the effects of anaerobiosis. On one hand, it stops aerobic decay processes (organic matter decay, nitrification). On the other, microbial populations begin to die off due to anaerobic factors.

For a given property, the variation caused by the biochemical cycle will be the sum of all the variations of related properties. For example, Nitrate is produced by Nitrification, and depleted by immobilization, denitrification, etc

$$\frac{\partial[\text{NO}_3^-]}{\partial t} = -\left(K_{\text{denitrification}} + K_{\text{immobilization}}\right)[\text{NO}_3^-] + K_{\text{nitrification}}[\text{NH}_4^+] \quad (2.3.4)$$

If Nitrate concentrations are plotted along a given period, a typical growth curve is obtained (*Figure 2.4- Generic property variation curves*). If the property's concentration is low, the sink term of (2.3.4) is small and the nitrate concentration will grow.

Has the concentration increases the sink term will have greater impact on the overall balance.

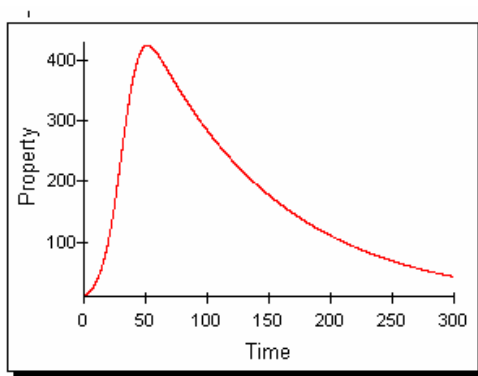


Figure 2.4- Generic property variation curves

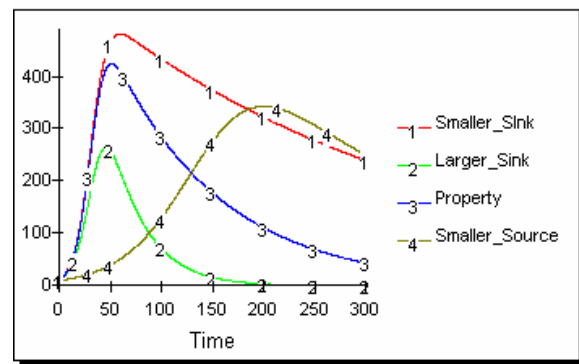


Figure 2.5- Effects of different specific rates

When the negative terms of (2.3.4) surpass the positive terms, the growth curve enters a declination period (*Figure 2.4*).

If the specific rates of the sink terms of (2.3.4) are augmented, the maximum point occurs for the same time *Figure 2.5 - (2) - (3)*, but with lower maximum concentrations and with greater decline in descendent phase (3).

If the sources terms are diminished, the maximum point will occur at a later time (*Figure 2.5 - (4)*). The Declines of the growth and descent phases are smoothen and the lag phase that precedes the initial growth is more evident.

2.3.2- Carbon Pools

All the models cited in *Chapter 2.2-Nitrogen Sources*, use different conceptual models for soil organic matter pools. Almost all of them divide soil organic matter into active, slow and passive fractions. However, the way organic matter passes from one compartment to another is modeled in completely different ways.

At this point, simplified compartments of SOM² were used. Two compartments, one of labile and one of refractory Organic matter, were conceived. Both have independent Carbon / Nitrogen ratios. When the microbial biomass dies, its Carbon and Nitrogen will go to the labile pool. No source terms exist for the refractory pool.

- Other carbon pools are:
- Heterotrophic Carbon
- Autotrophic Carbon
- Anaerobic Carbon

The Heterotrophic group includes three different types of organisms: soil fungi, aerobic bacteria, and the aerobic part of the facultative aerobic bacteria. The anaerobic part of this last group is referred as Anaerobic Carbon.

Heterotrophic Carbon accounts for aerobic bacteria, fungi, and the aerobic part of the facultative aerobic bacteria. If anaerobic conditions arise, Heterotrophic Carbon will be diminished while Anaerobic Carbon grows. No explicit simulation is made for facultative aerobic bacteria changing from aerobic processes to anaerobic ones. This would further diminish Heterotrophic Carbon and increase the anaerobic Carbon when transitions occur from dry to wet soil.

Autotrophic Carbon represents the Nitrifying bacteria *Nitrobacter*. *Nitrossomas* action and thus the production of nitrite is not modeled explicitly (*1.2.3-Nitrification*), so no accumulations of nitrite is considered.

2.3.3- Nitrogen Pools

The simulated Nitrogen pools will be:

- | | |
|----------------------|-----------------|
| • Ammonia | • Autotrophic N |
| • Nitrate | • Anaerobic N |
| • N gas (see 2.3.6-) | • Refractory N |
| • Heterotrophic N | • Labile N |

Soil microbes like other organisms, require a balance of nutrients from which to build their cells and extract energy (Brady et al. 2000). The majority of soil organisms metabolize carbonaceous materials both in order to obtain carbon for building essential organic compounds and to obtain energy for life processes.

² Soil Organic matter

However, they must also obtain sufficient Nitrogen to synthesize nitrogen containing cellular components, such as amino acids, enzymes and DNA. As so unless storage occurs, carbon and nitrogen uptake rates are intimately related.

The CN ratio of microbial biomass is represented in *Table 2.1*.

For simulation purposes a CN average of 8 (Brady et al. 2002) will be used for all microbial pools

Organic material	%C	%N	C/N
Hardwood sawdust	46	0.1	400
Sugarcane trash	40	0.8	50
Digested Municipal sewage sludge	31	4.5	7
Soil microorganisms			
Bacteria	50	10	5
Actinomycetes, nematodes	50	8.5	6
Fungi	50	0.5	10
Soil Organic matter			
Average forest O horizons	50	1.3	45
Average forest A horizons	50	2.5	20
Average B horizons	46	5.1	9

Table 2.1- Carbon / Nitrogen ratio of some soil Organic Materials (source Brady 2002)

2.3.4- Autotrophic processes

A good starting point for the cycle conceptualization is the autotrophic processes, since they are only limited by the available amount of NH_4^+ . The nitrification rate will be modeled by first order kinetics following the RZWQM specific rates formulation (2.2.5). In this case:

$$K_{nitrification} = f_{aer} \left(\frac{k_b T_{nitrification}}{h_p} A_{nitrification} \right) \exp \left(- \frac{E_a}{R_g T_{nitrification}} \right) \frac{[O_2]^{0.5}}{[\gamma_1 H]^{k_H}} Pop_{Autotrophs} \quad (2.3.5)$$

So the nitrification rate is defined by (2.3.6)

$$K_{nitrification} [NO_3^-] \quad [\mu g/day/m^3_{water}] \quad (2.3.6)$$

When the autotrophic organisms promote this transformation, they retain part of the denitrified Nitrogen to build their own cell components. This will lead to an increase of the autotrophic Nitrogen mass according to (2.3.7).

$$NEfficiency_{Autotrophic} K_{nitrification} [NO_3^-] \frac{m_{water}^3}{kg_{soil}} \quad (2.3.7)$$

$$[\mu g/day/m_{water}^3]$$

In order to maintain their delicate Carbon / Nitrogen balance, the autotrophic biomass must uptake eight times the value of (2.3.7) in Carbon. Since Autotrophs use CO_2 as a Carbon source, Nitrification depletes the soils atmosphere of this gas. At the current stage of development, soil CO_2 will be considered none limiting, so the Autotrophic microorganisms will vary their carbon content according to (2.3.8)

$$NEfficiency_{Autotrophic} K_{nitrification} [NO_3^-] \frac{m_{water}^3}{kg_{soil}} \frac{1}{CN_{autotrophs}} \quad [\mu gC/day/kg_{soil}] \quad (2.3.8)$$

Where $CN_{autotrophs}$, represents the carbon / nitrogen ratio of the autotrophic biomass. No excretions of either Carbon or nitrogen are assumed.

2.3.5- Heterotrophic processes

Heterotrophic biomass can be considered as the start engine of the whole Nitrogen cycle, since they turn the nitrogen contained in the organic residues into their own biomass and later into ammonia.

This process can be limited by the availability of either Nitrogen or Carbon. If no mineral Nitrogen immobilization occurs (1.2.2-Immobilization) the microbial growth is only limited by the amount of available carbon. On the other hand, if mineral N is immobilized, the difference between the Organic Matter and Nitrogen immobilization rates will decide the limiting factor.

The potential (if no N limitation occurs) Organic matter decay rate if modeled according to (2.3.9)

$$K_{labileOM} [LabileCarbon] \quad \mu g/day/kg_{soil} \quad (2.3.9)$$

$$K_{labileOM} = f_{aer} \left(\frac{k_b T_{labileOM}}{h_p} A_{labileOM} \right) \exp \left(- \frac{E_a}{R_g T_{labileOM}} \right) \frac{[O_2]}{[\gamma_1 H]^{K_H}} Pop_{Heterotrophs} \quad day^{-1} \quad (2.3.10)$$

Only two organic matter pools were modeled, a labile one and a refractory one. Equations (2.3.9) and (2.3.10) are for the labile pool, but are also applied to the refractory pool except in this case different coefficients are used for A and E_a . Equation (2.3.9) is for the Organic matter Carbon decay. Assuming a uniform distribution within the organic matter, organic Nitrogen decay equals (2.3.9), times the inverse of the organic matter Carbon / Nitrogen ratio.

For Nitrogen, immobilization specific rates similar to (2.3.10) are used (again with different coefficients). The Ammonia and Nitrate immobilization rates are:

$$K_{Ammonia} [NH_4^+] \quad \mu g/day/m^3_{water} \quad (2.3.11)$$

$$K_{Nitrate} [NO_3^-] \quad \mu g/day/m^3_{water} \quad (2.3.12)$$

The ammonia specific immobilization rate is greater than the Nitrate one. Since Nitrogen is more easily segregated from the Hydrogen molecule than from oxygen.

The comparison of (2.3.13) and (2.3.14), defines the limiting factor.

$$(I_{NH_4^+} + I_{NO_3^-}) * \frac{m^3_{water}}{kg_{soil}} \quad [\mu g/day/kg_{soil}] \quad (2.3.13)$$

$$P_{LC} \left(\frac{1}{CN_{Heterotrophs}} - \frac{1}{CN_{labile}} \right) + P_{RC} \left(\frac{1}{CN_{Heterotrophs}} - \frac{1}{CN_{refractory}} \right) \quad [\mu g/day/kg_{soil}] \quad (2.3.14)$$

$I_{NH_4^+}$ is the potential ammonia immobilization rate, defined by (2.3.11), $I_{NO_3^-}$ is the same for Nitrate, defined by (2.3.12). The potential rates for refractory and labile Organic matter decay are represented by P_{RC} and P_{LC} . Heterotrophic and Organic matter pools Carbon / Nitrogen ratio are expressed as, $CN_{Heterotrophs}$, CN_{Labile} and $CN_{refractory}$.

Equation (2.3.13) represents the possible Nitrogen immobilization at the maximum (potential) rate. Equation (2.3.14) translates the Nitrogen needs of the Heterotrophic biomass if the organic matter was consumed at the potential (maximum) rate.

If (2.3.14) is smaller than (2.3.13) the organic matter potential decay is the limiting factor and will control the mineral Nitrogen immobilization rate as well as the Heterotrophic population growth. Assuming that these new immobilization rates keep the same proportion that the potential ones had, the real Ammonia $RI_{NH_4^+}$ and Nitrate Immobilization $RI_{NO_3^-}$ rates can be calculated by (2.3.15) and (2.3.16).

$$RI_{NH_4^+} = \left[P_{LC} \left(\frac{1}{CN_{Heterotrophs}} - \frac{1}{CN_{labile}} \right) + P_{RC} \left(\frac{1}{CN_{Heterotrophs}} - \frac{1}{CN_{refractory}} \right) \right] \frac{1}{Partition + 1} \quad (2.3.15)$$

$$RI_{NO_3^-} = \left[P_{LC} \left(\frac{1}{CN_{Heterotrophs}} - \frac{1}{CN_{labile}} \right) + P_{RC} \left(\frac{1}{CN_{Heterotrophs}} - \frac{1}{CN_{refractory}} \right) \right] \frac{1}{1/Partition + 1} \quad (2.3.16)$$

Where:

$$Partition = \frac{K_{nitrate} [NO_3^-]}{K_{ammonia} [NH_4^+]} \quad (2.3.17)$$

On the other hand if (2.3.13) is smaller than (2.3.14) the nitrogen immobilization rates will control the organic matter decay and consequent microbial growth. Once again, a constant proportion was assumed for the labile and refractory matter decay. The labile and refractory decay rates, RP_{labile} and $RP_{refractory}$ are modeled by (2.3.18) and (2.3.19).

$$RP_{labile} = \frac{I_{NO_3^-} + I_{NH_4^+}}{\left(\frac{1}{CN_{Heterotrophs}} - \frac{1}{CN_{labile}} \right) + Partition \left(\frac{1}{CN_{Heterotrophs}} - \frac{1}{CN_{refractory}} \right)} \quad (2.3.18)$$

$$RP_{refractory} = \frac{I_{NH_4^+} + I_{NO_3^-}}{\left(\frac{1}{CN_{Heterotrophs}} - \frac{1}{CN_{labile}} \right) 1/Partition + \left(\frac{1}{CN_{Heterotrophs}} - \frac{1}{CN_{refractory}} \right)} \quad (2.3.19)$$

In this case:

$$Partition = \frac{K_{refractory} [ROMC]}{K_{labile} [LOMC]} \quad (2.3.20)$$

Not all of the decayed biomass will be used for Heterotrophic growth. Most of it will be lost as CO_2 according to predefined carbon efficiency. The Heterotrophic Carbon growth is translated by:

$$TotalC_{decay} Het_{efficiency}^C \quad (2.3.21)$$

The same is assumed for Heterotrophic Nitrogen:

$$\left(TotalOMN_{decay} + TotalN_{immobilization} \right) Het_{efficiency}^C \quad (2.3.22)$$

In nature, the process of nitrogen mineralization involves the entire food web, and not just the saprophytic bacteria and fungi that are represented in the model as heterotrophic biomass.

Certain nematode, protozoa and earthworms feed on the saprophytic biomass. As these animals feed, they respire most of the carbon in the microbial cells, using only a small fraction to grow on (or produce eggs). Since the C/N ratio of these animals is not too different from that of their microbial food, and most of

the carbon is converted to CO_2 , the predators must excrete most of the ingested nitrogen as ammonia. According to Brady et al 2002 this bacterial feeding activity of soil animals may increase the rate of nitrogen mineralization by 100%.

Even though the importance of predation in nitrogen mineralization is undeniable, a simple approximation may prove good results, since the accumulation of cycle elements by the predatory biomass is negligible. As so at this point, the assumed breathe and ammonia excretion rates ((2.3.21) and (2.3.22)) simulate both the Heterotrophs efficiency and the predatory effects. This means that the predatory effects are modeled with first order kinetics without explicit predatory biomass and as so without variations of the predatory specific rate. This should be a point to consider in future work.

2.3.6- Anaerobic processes

The denitrification rate follows (2.3.23)

$$K_{Denitrification} [NO_3^-] \quad [\mu g/day/m^3_{water}] \quad (2.3.23)$$

$$K_{Denitrification} = f_{anaer} \left(\frac{k_b T_{Denitrification}}{h_p} A_{Denitrification} \right) \exp \left(- \frac{E_a}{R_g T_{Denitrification}} \right) \frac{[O_2]}{[\gamma_1 H]}^{k_H} Pop_{Anaerobic} \quad (2.3.24)$$

During the denitrification processes the anaerobic biomass will retain part of the Nitrogen and release the remaining in gaseous forms of Nitrogen (N_2 , N_2O) according to a predefined Nitrogen efficiency. At this point no distinguish is made between any of the gaseous forms of Nitrogen. Instead a unique property (N_{gas}) is assumed.

Since Nitrate is used as an alternative oxidant for the Organic matter, the decay of Labile and refractory carbon are evaluated from the denitrification rate. Shaffer et al. 1995 proposes a factor of 0.1 to perform this conversion.

$$K_{Denitrification} [NO_3^-] \frac{m^3_{water}}{kg_{soil}} \frac{\mu g C}{\mu g NO_3^-} \quad [\mu g/day/kg_{soil}] \quad (2.3.25)$$

If Nitrate supplies are low, hydrogen can be used as an alternative oxidant, giving off carbon in respiration in the form of methane. At this point, this still is not implemented.

The Anaerobic Carbon efficiency was considered equal to the Aerobic one so (2.3.25) can be portioned into a labile and refractory Carbon decay.

Assuming that the Anaerobic and aerobic decay rates are proportional in each pool, labile Carbon decay is:

$$LabileC_{decay} = \frac{m_{water}^3}{kg_{soil}} \frac{\mu g C}{\mu g NO_3^-} K_{Denitrification} [NO_3^-] \frac{1}{Partition} [\mu g/day/kg_{soil}] \quad (2.3.26)$$

Partition is defined by (2.3.20).

For Refractory Carbon decay (2.3.26) is valid except for the partition term where $\frac{1}{1/Partition + 1}$ will be used.

Organic nitrogen uptakes are modeled by the respective pool (labile or refractory) decay rate times the inverse of the respective Carbon / Nitrogen ratio.

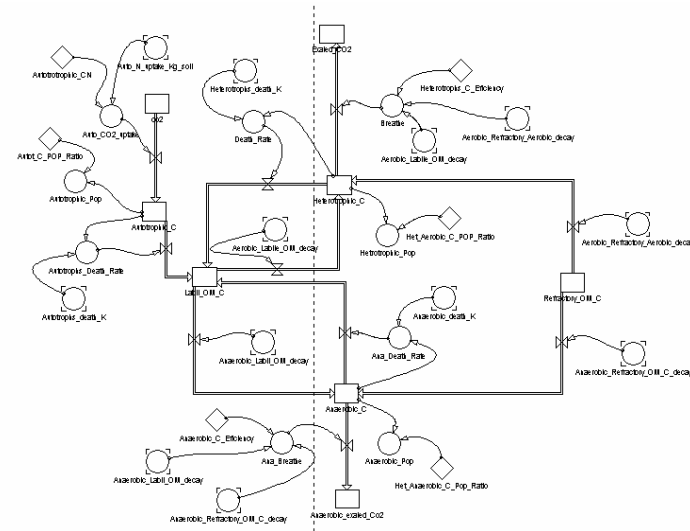
A Nitrogen balance is obtained between the obtained Nitrogen and Carbon. Using the nitrogen efficiency proposed by Shaffer et al. 1995, unless organic matter pools have CN³ ratios as high as 200, no Anaerobic Nitrogen immobilization is required. No data was found in the literature that verified or rejected this theory. As so, in this model, anaerobic pathways are intrinsically mineralizing. Anaerobic Nitrogen excretions are represented by (2.3.27).

$$Anaerobic_{excretion} = K_{denitrification} [NO_3^-] * \left(\begin{array}{l} \frac{Ratio_{OM/NO_3^-}}{(Partition + 1)CN_{labil}} + \frac{Ratio_{OM/NO_3^-}}{(1/Partition + 1)CN_{refract}} \\ + efficiency - \frac{Ratio_{OM/NO_3^-}}{CN_{Anerobic}} \end{array} \right) [\mu g NH_4^+/day/m_{water}^3] \quad (2.3.27)$$

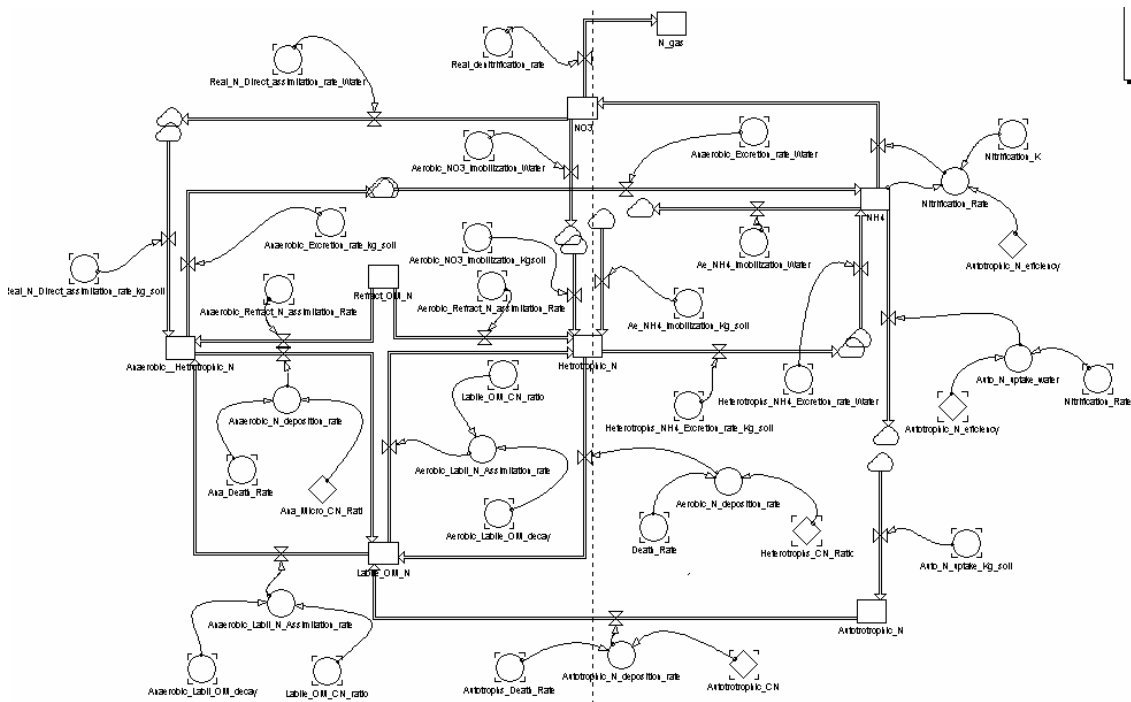
³ Carbon / Nitrogen

2.3.7- Global balance

After all these equations and interspecies relations were implemented, the global carbon cycle resembles



And the same for nitrogen cycle



2.4- POWERSIM analysis

A good example of this model versatility is demonstrated with a simple immobilization test. Initial Carbon and Nitrogen pools were established for values similar to those presented by Cameira, 1998, except for the Organic Nitrogen values:

Nitrogen Pools		Carbon Pools	
Ammonia	$7 [g\ kg_{soil}^{-1}]$	Heterotrophic Carbon	$105.26 [\mu g\ g_{soil}^{-1}]$
Nitrogen	$0 [g\ kg_{soil}^{-1}]$	Autotrophic Carbon	$0.11 [\mu g\ g_{soil}^{-1}]$
Heterotrophic Nitrogen	$18.78 [\mu g\ g_{soil}^{-1}]$	Anaerobic Carbon	$1.05 [\mu g\ g_{soil}^{-1}]$
Autotrophic Nitrogen	$0.138 [\mu g\ g_{soil}^{-1}]$	Labile Carbon	$581.12 [\mu g\ g_{soil}^{-1}]$
Anaerobic Nitrogen	$0.131 [\mu g\ g_{soil}^{-1}]$	Refractory Carbon	$23244.78 [\mu g\ g_{soil}^{-1}]$
Labile Nitrogen	$581.12 [\mu g\ g_{soil}^{-1}]$		
Refractory Nitrogen	$2905.6 [\mu g\ g_{soil}^{-1}]$		

Table 2.2- Carbon and Nitrogen Pools initialization

This system is placed under heavy Nitrogen stress. The Carbon / Nitrogen ratio of the residues is different from that of the soil fauna (CN of labile OM is as high as 100).

At this first simulation, the soils water levels were considered constant at an aerobic level.

The variation of the different Nitrogen pools are represented in *Figure 2.6 - Year long Nitrogen variations*

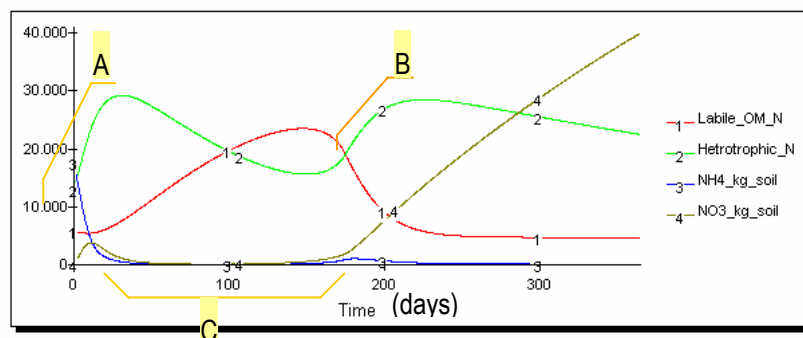


Figure 2.6 - Year long Nitrogen variations

There are clearly two different growth phases for the Heterotrophic biomass. For the first one (A), Heterotrophic Nitrogen (2) is growing, but so is the labile Organic Matter Nitrogen content (1). On the other hand, all the mineral Nitrogen forms (3, 4) disappear from the system, due to Heterotrophic incorporation.

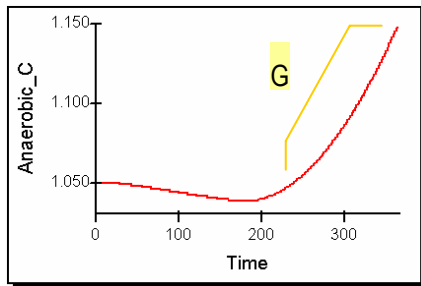


Figure 2.7 – Anaerobic growth curve

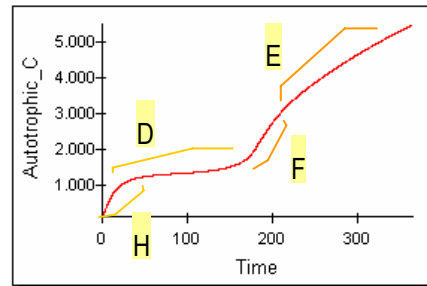


Figure 2.8- Autotrophic growth curve

This yields a Nitrogen depression period during which mineral Nitrogen will not be available for soil flora. All the NH_4^+ produced during this period is quickly immobilized by Heterotrophic action. Very little ammonia is available for Nitrification, limiting Autotrophic growth *Figure 2.8 (D)*.

It is interesting to note that some competition, between Heterotrophs and Autotrophs for the available Ammonia, occurs in the initial period resulting in some Autotrophic growth *Figure 2.8 – (H)*. However, Heterotrophic biomass soon retains most of the Ammonia. Some Nitrate production occurs at residual rate, but Heterotrophic Immobilization quickly drains the soil of this Nitrogen form.

In *Figure 2.6*, Labile Nitrogen is increasing due to biomass death. Microorganism's biomass returns more Carbon than Nitrogen when death occurs. Organic labile Nitrogen is depleted at a reason of 1 part of Nitrogen for each 100 parts of Carbon and is supplied with a reason of 1 part for each eight parts of Carbon, leading to a reduction of labile CN *Figure 2.9*. In a global perspective, Nitrogen is conserved (denitrification rates are negligible), while Carbon is lost by respiration. Some carbon input exists due to the Autotrophic processes, but this incorporation is much less than Heterotrophic respiration (Heterotrophic populations are 100 times the Anaerobic ones.)

The death phase that follows the initial growth period *Figure 2.3 - (A)* is due to Nitrogen limitation. There's not enough mineral Nitrogen to supply the existing Heterotrophic population. However, labile Organic matter CN is getting close to a point where Mineral Nitrogen immobilization won't be limiting.

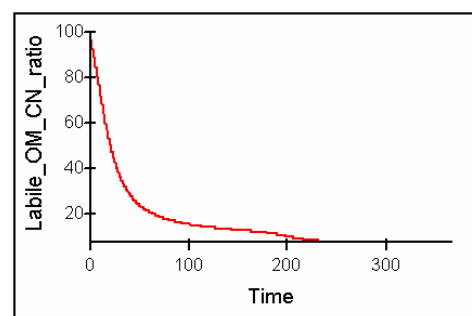


Figure 2.9 - Labile OM CN ratio variations

At this point (labile CN near 20) the Heterotrophic Ammonia excretion rate will surpass the Immobilization rate. Immobilization is still needed, but Ammonia levels will grow. This leads to a situation where Ammonia Immobilization increases its own rate. The more Heterotrophs immobilize, the faster they grow, more ammonia is produced and more they can immobilize which in turn leads to higher Heterotrophic growth

rates. The initial period of curve *Figure 2.6 - (B)* correspond to this situation. Autotrophic growth also responds to these ammonia increases *Figure 2.8 - (F)*.

Soon the carbon uptake rate will be the limiting factor and the second growth period *Figure 2.6 - (B)* takes place. At this stage more ammonia is produced than immobilized, so Autotrophs can nitrify *Figure 2.8 - (E)*. This leads to increasing concentrations of Nitrate, and soon some minimum anaerobic denitrifying activity will take place *Figure 2.7 - (G)*.

Repeating the same simulation with and initial labile CN of 20, no Nitrate depression period occurs. Only one Heterotrophic growth curve is present *Figure 2.10*.

For intermediate CN ratios, both Heterotrophic maximums grow apart and the Nitrate depression period increases (*Figure 2.10*).

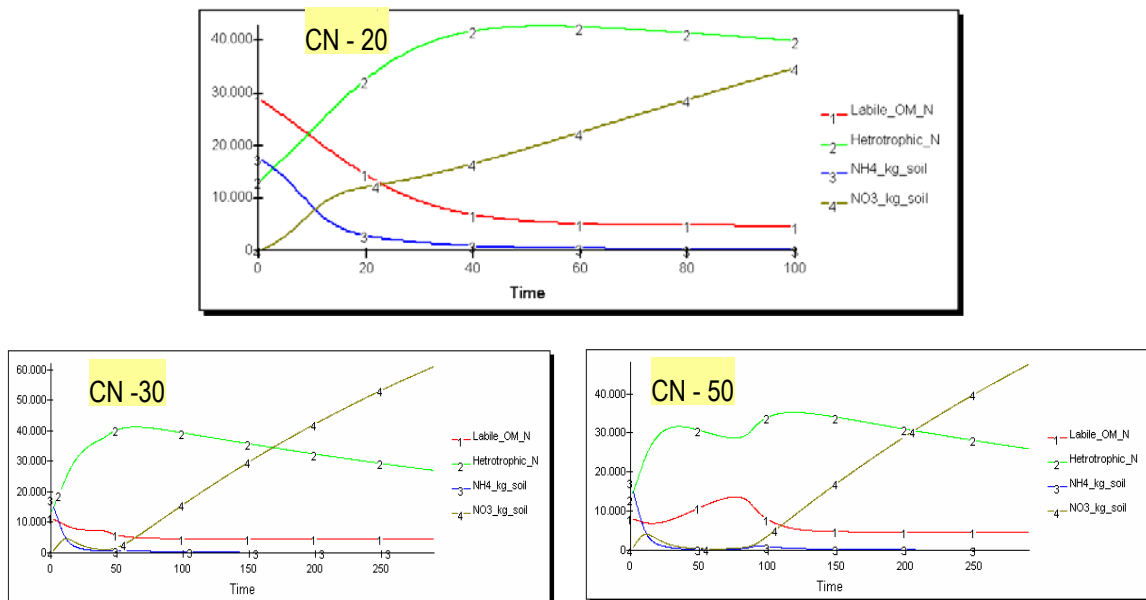


Figure 2.10- Cycle variations with Labile CN

If Nitrogen stress is greater than a maximum value only one maximum may be present. Refractory Nitrogen also affects the Heterotrophic growth curves distribution, but with less intensity.

Repeating the initial simulation with greater water content, anaerobic processes gain importance and Nitrogen gas is produced. However this is a slow and ineffective process that takes much longer to obtain large concentrations of Nitrogen gas *Figure 2.11*.

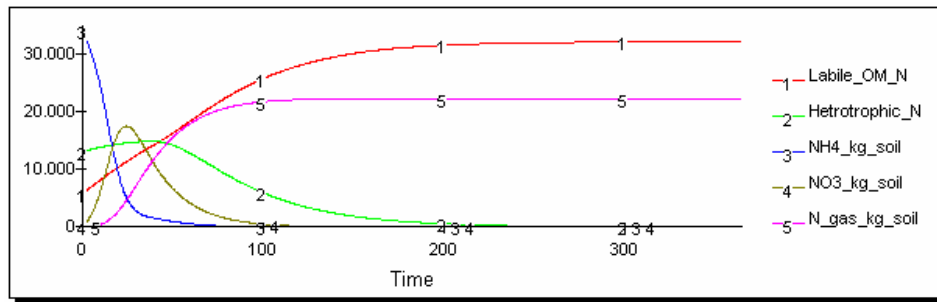


Figure 2.11-Anaerobic condition

Some Nitrogen immobilization occurs before Heterotrophic biomass begins to die off. When this happens, Ammonia excretions begin to nitrify and Nitrate is produced. However, the initial levels of Mineral Nitrogen are never replaced.

Comparison of the situations represented in *Figure 2.11* and *Figure 2.6*, illustrates the effect of soil water contents on the soils microorganisms.

Another very important effect of soil water is the direct effect on the properties concentrations. The only dissolved properties are the Ammonium and Nitrate ions. If for some reason soil water content drops to half, the Ammonia immobilization rate $[\mu\text{g kg}_{\text{soil}}^{-1}]$ will remain the same. However, the nitrification $[\mu\text{g m}_{\text{water}}^{-3}]$ rate will be doubled, giving an advantage to the nitrifying bacteria. Heterotrophic biomass will immobilize the Nitrate anyway, but the immobilization rate is smaller for Nitrate than for Ammonia. As so variations of soil water content can change the Heterotrophic growth's limiting factor from Carbon to Nitrate.

At this point POWERSIM limitations begin to appear. The only way to change a state variable value is thru a mass flux. For instance, ammonia concentration can only change if some ammonia turns into Nitrate. Ammonia and Nitrate concentrations cannot increase when dryness episodes occur.

2.5- FORTRAN implementation

In the MOHID structure, the previously implemented SEDIMENTPROPERTIES module controls the evolution of properties in the sediments. Partitions processes, advection – diffusion processes are all controlled by this module.

In order to include sediment processes in MOHID, some new modules were added to the modular structure. The model's philosophy and hierarchy can be seen has in the picture below.

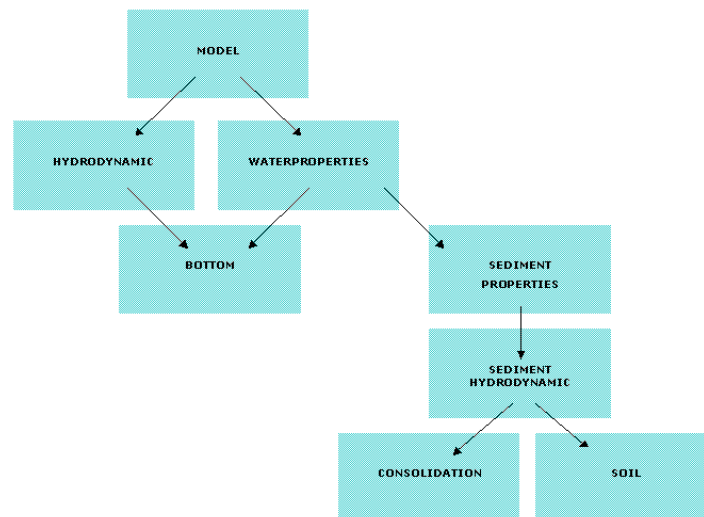


Figure 2.12- MOHID's general Hierarchy

SEDIMENTPROPERTIES is a client of WATERPROPERTIES. Therefore, if one specifies that a certain water property should be computed with sediments processes, the SEDIMENTPROPERTIES module is coupled. Two distinct water flow models are available to this module, a soil water flow model and a consolidation model. The use of these two hydrodynamic modules is managed by an interface, SEDIMENTHYDRODYNAMIC.

If any given property has sediments processes enabled, module SEDIMENTPROPERTIES calls module ADVECTIONDIFFUSION to calculate mass transport within the sediments. Module SEDIMENTHYDRODYNAMIC supplies the water fluxes and volumes needed for the module ADVECTION DIFFUSION to function (see *APPENDIX II*).

SEDIMENTPROPERTIES, will calculate the diffusion coefficients and partition processes, and will store and output the properties concentrations. Finally, it calculates the mass flux between sediments and the water column.

For the Carbon / Nitrogen cycle in soil, a new module was created, SEDIMENTQUALITY, this module will solve the system of differential equations presented in chapter *2.3.1-Model conceptualization*.

A private subroutine was created in SEDIMENTPROPERTIES, to use SEDIMENTQUALITY. This routine uses MODULEINTERFACE to transform the cycle element's concentrations in the three dimensional domain into uni-dimensional arrays (one for each property). Each line of this array corresponds to certain cell. These uni-dimensional arrays are grouped in a matrix (*Figure 2.13*) and supplied to SEDIMENTQUALITY, which in turn runs through every column in the newly formed array calculating new properties concentrations.

$$\begin{bmatrix} \text{First property} & \text{FirstCell} & \text{SecondCell} & \dots & \text{LastCell} \\ \vdots & \vdots & \dots & \dots & \vdots \\ \text{Last property} & \text{FirstCell} & \dots & \dots & \text{LastCell} \end{bmatrix}$$

Figure 2.13 - Example of SEDIMENTQUALITY array

After SEDIMENTQUALITY's calculations, the newly obtained concentrations will be returned to SEDIMENTPROPERTIES, after MODULEINTERFACE turns the concentrations array back into several three-dimensional arrays, one for each property.

SEDIMENTPROPERTIES also has to coordinate the different time steps that each process needs. Soil hydrodynamic, due to the shape of the matric potential – water retention curve, needs a variable time step (*APPENDIX I*). If wet soil is in contact with dry soil massive gradients are present, and minor steps are needed to assure stability. When matric potential gradients are smaller, MODULESOIL increases the time step so that computation time is reduced.

For a good soil hydraulics computation, the maximum time step is usually around 50 seconds, depending on the soil type. For cycle processes, larger time steps are used. The typical, time interval used is about 6 hours. SEDIMENTPROPERTIES conjugates these different time steps, paying attention only to the smaller one (soil). New concentrations calculated by SEDIMENTQUALITY, are divided by the module's time step (six hours) and multiplied by this minimum time step, every time the soil's hydrodynamics is calculated. When enough time has passed, SEDIMENTQUALITY is called again and the process restarts.

2.5.1- System Solution

Up to this point, no attention was paid to numerical solutions for the equations presented in *Chapter 2.3*-. Such equations can be solved with an explicit approach or an implicit approach. The explicit approach has the advantage of being quicker and simple to program. On the other hand, the implicit method has the reputation of maintaining stability for larger time steps. If an explicit approach is used, all the cycle equations will be discredited according to (2.5.1).

$$c_j^{t+\Delta t} = c_j^{t+\Delta t} + \Delta t \sum_{j=1}^{pn} K_i c_i^t \quad (2.5.1)$$

Where c represents a generic property, K_i is the specific rate for pool i , Δt is the chosen time step and pn is the total properties number. This is a very simple system to solve since all the terms on the right hand side are known.

If an implicit method is chosen, equation (2.5.2) will be solved.

$$c_j^{t+\Delta t} = c_j^t + \Delta t \sum_{i=1}^{pn} K_i c_i^{t+\Delta t} \quad (2.5.2)$$

In order to obtain the new properties concentration, a matrix inversion process must be involved (in MOHID, this is performed in module LUD). Also some explicit nature must be present, since all the specific rates K depend on some properties. If these properties were evaluated at $t + \Delta t$, equation (2.5.2) would not be linear, leading to a system of difficult resolution.

A third method was implemented in MOHID, a “semi-implicit” method. This method uses a peculiar approach to numerical problems that may arise from the remaining two methods.

Since all the processes have an exponential analytic solution, the properties evolution curves should follow. The explicit method uses “old” concentrations to evaluate the new ones this is a good approximation for exponential growth terms since the numerical solution is always inferior to the analytical one. On the other hand for exponential decay (that correspond to sink sources), the numerical solution may lead to negative values (meaningless for concentrations).

The implicit method behaves in an opposite manner, since new concentrations are evaluated from themselves, new concentrations are always over estimated. This never leads to negative values, but may cause numerical instability due to excessive large numbers in source terms.

In the semi-implicit method if a term is a source it will be solved by an explicit method, on the other hand if it is a sink term, an implicit method is used, according to (2.5.3).

$$c_j^{t+\Delta t} = c_j^t + \Delta t \sum_{i=1}^{pn} E_i c_i^t + \Delta t \sum_{i=1}^{pn} I_i c_i^{t+\Delta t} \quad (2.5.3)$$

If the specific rate is positive, E_i equals it and I_i is null. The opposite is true for sink terms.

This method has advantages in terms of stability, however since the same term can be a sink in the evolution equation of a given property and simultaneously a source for another property, mass conservation issues will arise.

2.5.2- General Module Structure

In SEDIMENTQUALITY, specific rates calculation, the relations between cycle properties and the resolution of the obtained system of equations, are all separate processes. With such an approach, new kinetics can easily replace the used one and new properties or processes can be added without major changes to the existing program's code.

This module receives the array described in 2.5-FORTRAN *implementation*, and runs through every column.

The Dissolved oxygen is calculated according to Henry's law (according to Metcalf and Eddy (1978)), using the cells temperature.

In the next step the anaerobic ($f_{anaerobiose}$) and aerobic ($f_{aerobiose}$) functions of (2.3.1) are calculated. The method of Caskey and Scheppers, 1985 as in Shaffer et al 19995 is used.

According to Shaffer et al. 19995, when soil water content is high conditions are strongly anaerobic. The opposite holds at low water content. The assumption for this is that the higher oxygen content of the soil atmosphere raises the dissolved oxygen concentration in the interstitial water.

As so, the values of the factors $f_{anaerobiose}$ and $f_{aerobiose}$ are related to the percentage of the soil's interstitial space filled with water. This quantity is calculated in SEDIMENTHYDRODYNAMIC and passed by argument into SEDIMENTQUALITY.

Table 2.3 summarizes the relation between $f_{anaerobiose}$, $f_{aerobiose}$ and the percentage of water -filled pore space

θ_{rf}	$f_{aerobiose}$	θ_{rf}	$f_{anaerobiose}$
60	1.00	60	0.001
70	0.40	80	0.130
80	0.10	100	1.000
87	.001		

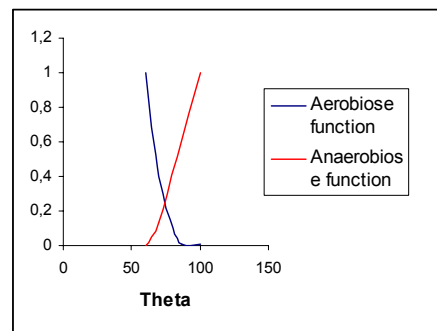


Table 2.3- Relation between aerobic and anaerobic coefficients and the percentage of water filled space

Figure 2.14-Aerobic and anaerobic coefficients of as a functions of the percentage of water filled pore space

The next step is to calculate all the specific rates, according to the user supplied coefficients and (2.3.1). Tests are made to evaluate the necessity of mineral Nitrogen immobilization and the limiting factors for Heterotrophic action are established see chapter 2.3.1-Model conceptualization.

A matrix is assembled these coefficients, that correspond to the specific rate times the time interval (see 2.5.1-System Solution). Using this array and the current concentrations has the independent term, the new values for each property are calculated (2.5.1-System Solution).

Then the module moves to the next cell and the process restarts.

2.5.3- Initial Results Analysis

The first analysis performed on MOHID were to compare FORTRAN results with POWERSIM.

If programming error occurred both results would be different.

In order for both results (POWERSIM and MOHID) to be directly comparable, MOHID soil hydrodynamics' was disconnected through the use of very low conductivities (as low as $10E-60$).

In this particular case, when the nitrate depression period is over, most of the labile carbon has already been consumed. Transitions from carbon to nitrogen limitation by the Heterotrophic biomass are also verified and as so this is a good test run for the different subroutines used by SEDIMENTQUALITY.

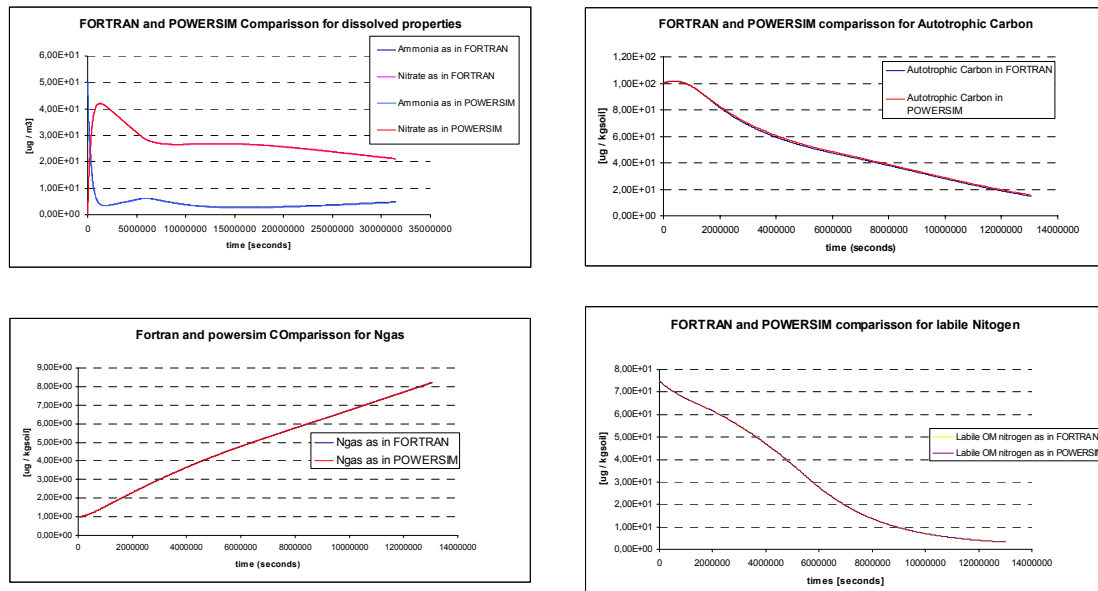


Figure 2.15- POWERSIM – FORTRAN comparison

Both models produced a similar result, which verifies the consistency between them. The depression period is present and leads to two different growth curves. In both situations (Nitrogen and Carbon limitation), the different models responded in a similar fashion.

MOHID can output results in two different formats, time series in ASCII format or HDF. Time series correspond to the variation of one or several properties, along the simulation time, in a given cell.

In HDF- Hierarchical Data Format, a single property values are outputted in all the domain cells, for each instant. MOHID graphic user interface recognizes this format and allows several representations such as isolines, vector field, etc.

The graphics presented on this page are the result of time series. In order to save time, a Microsoft Excel macro was developed to read the ASCII data, from the outputted time series of both POWERSIM and MOHID and create these graphics. More information about these macros can be found in (APPENDIX IV).

For multidimensional test, more data must be gathered. In all of the runs that are presented in this chapter, hydraulic properties from a soil in Alvalade (Alentejo) was used, since this data was available (Chabel-Leitão et al. 2002).

Actual climatological data from Alvalade was also used. Precipitation and evaporation, data were gathered from May 2001 to the same month in 2002 *APPENDIX III*.

3.1- Simple soil column

Nitrogen dynamics was applied to the same soil column described in Chanbel Leitão et al. 2003, (see *APPENDIX III*). The different Carbon and Nitrogen pools were initialized in a uniform manner according to the values presented in *Table 2.2- Carbon and Nitrogen Pools initialization*.

A simple vertical discretization of 20 layers of 0.5 centimeters each was used. For horizontal discretization, a single cell of one square meter was defined, thus producing a one-dimensional model.



Figure 3.1- Vertical discretization

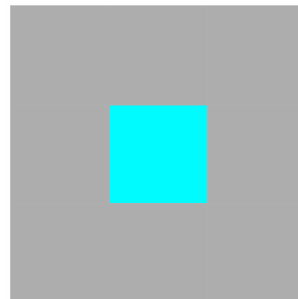


Figure 3.2- Horizontal grid

The grey cells in *Figure 3.2- Horizontal grid* are points that are out of the calculation domain. The boundary conditions for the bottom flux are of Newman type with null gradient.

Since the nitrogen ratio of the available residues is once again very low, all the available mineral nitrogen is immobilized in the first days of the simulations, like in chapter 0

POWERSIM analysis. However, variations of water content in depth will affect microbial action.

As *Figure 3.3- Water Content variations* shows, the water level variations are attenuated with depth. The opposite occurs with water content, which increases with depth.

Aerobic microbial biomass at the surface has to survive more water content variations. On the other hand, in deeper sections anaerobic conditions begin to appear, thus limiting aerobic processes.

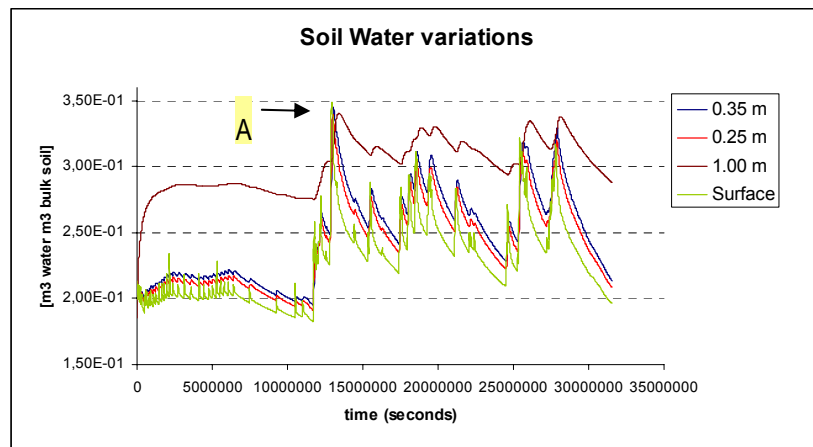


Figure 3.3- Water Content variations

Water velocity is also higher for the upper layers, which leads to higher transport velocities for dissolved properties. This poses an interesting question for the aerobic biomass, since it must balance the anaerobic conditions, dissolved properties leaching and water level variations.

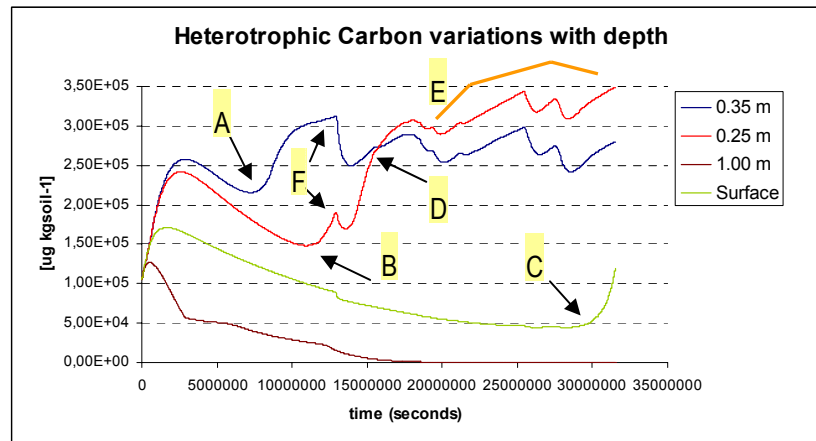


Figure 3.4- Heterotrophic Carbon Variations

From the analysis of *Figure 3.4*, two growth periods for the Heterotrophic population line are identified. The transition from nitrogen to carbon limitation occurs at different times (*Figure 3.4 – (A)(B)(C)*). For the surface cell, the heterotrophic population only enters a carbon-limited growth at the end of the run (*Figure 3.4 – (C)*). For 0.35 meters of depth, the transition occurs around September (*Figure 3.4 – (A)*). For 0.25 meters, a few months later (*Figure 3.4 – (B)*), and for the maximum simulated depth no transition occurs.

The transitional period is also visible in a dissolved ammonia plot, since ammonium ion concentrations have a small increase (*Figure 3.5 – (B)*) when transition for nitrogen to carbon occurs (response time for the autotrophic biomass to begin to nitrify see *Chapter 2.4- POWERSIM analysis*).

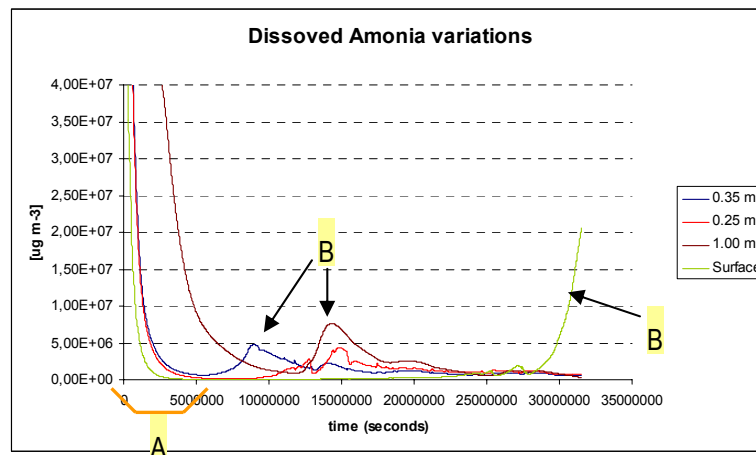


Figure 3.5- Dissolved Ammonia Variations

The initial variations of dissolved ammonia on the three upper cells, *Figure 3.5– (A)*, are quite similar, but the deeper the layer is the longer it takes to lower the ammonia concentration. In the initial period Heterotrophic populations are similar for all layers, so this variation is due to water transport from the upper layers to the lower ones. This conclusion is not valid for the final layer of 1.00 meters since strong anaerobic conditions are present from the beginning, thus lowering heterotrophic immobilization from the start.

The lower the values of mineral nitrogen are for a given cell, the longer the nitrate depression period will be (see *Chapter 2.4- POWERSIM analysis*), which would explain why surface populations suffer such a long depression period. However, the variations of ammonia are not enough to explain such differences as those experienced by Heterotrophic populations at the surface, and the next two layers.

A possible answer to this puzzle is the dissolved nitrate concentrations. During the nitrate depression period commented in *Chapter 2.4- POWERSIM analysis*, no nitrate increases occur. However, Aerobic populations never cease to grow *Figure 2.8 – (D)*. This indicates that some Nitrogen production occurs, but the nitrogen starved Heterotrophic biomass rapidly immobilizes the newly produced nitrogen. When the same situation occurs in this example, heterotrophic microorganisms will have more difficulty to immobilize Nitrate since water will leach it to deeper layers.

Figure 3.7. shows the variation of the Ammonium ion concentration without nutrient cycling. Variations are lower for deeper layers since the deeper the layer is, the smaller the water velocities are. In addition, all of the above layers will provide a source of dissolved properties.

As so, nitrate produced in the upper layers is washed to the lower ones, depriving aerobic biomass from its limiting factor. This allows the aerobic Heterotrophic biomass to surpass the nitrate depression period before the other layers.

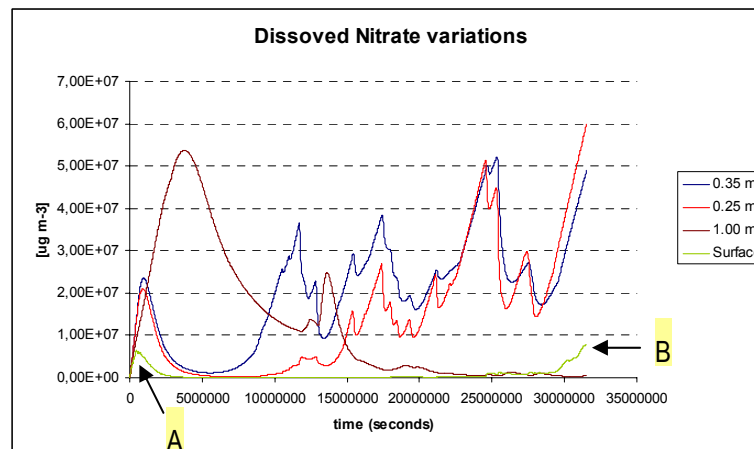


Figure 3.6- Nitrate Variations

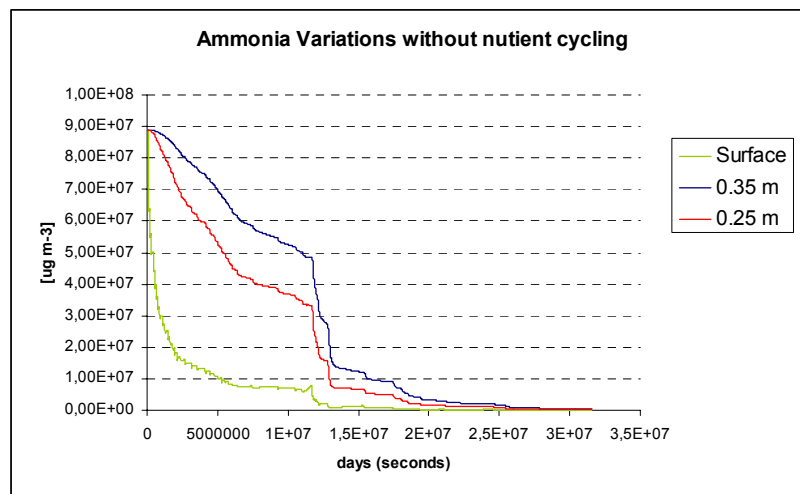


Figure 3.7- Ammonia Leaching without nutrient cycling

Once the nitrate depression period is over, Heterotrophic growth is only limited by the soil's carbon content. When this happens the cell with less total water content will have the higher population, unless occasional episodes wash away the minimum needed mineral nitrogen (even though it is a carbon-limited growth minor immobilization usually takes place). As so, the aerobic heterotrophic biomass at 0.25 centimeters soon surpasses the concentration at 0.35 (Figure 3.4 – (D)). From then on, population variations for these cells are parallel (Figure 3.4 – (E)), proportionally to their total water volume.

Another interesting event to note is the different effect that the soil water peak represented in Figure 3.3 – (A) has on the different layers heterotrophic growing curve (Figure 3.4 – (F)). For the cell at 0.35 centimeters, this variation happens at the stationary phase, when growth and death rates are in balance.

In this case, the anaerobic conditions produced, disrupt the balance situation and results in visible variations of the growth curve. For the higher layer, the same water variation occurs in the growth phase when growth rates far exceed the death rates. In this case, the increase of water content produces minor variations. For the surface layer, death rates are already higher then the growth rates and the water content variations produced no visible results.

After de depression period, Ammonia levels in the upper layer *Figure 3.5 – (B)* reach much higher levels than the remaining cells ever did. This also corresponds to low Nitrate production *Figure 3.6 – (B)*. The reason is that the long depression period, killed most of the Autotrophic population and as so a longer reestablishment time (during which little nitrification occurs) for the autotrophic population is needed.

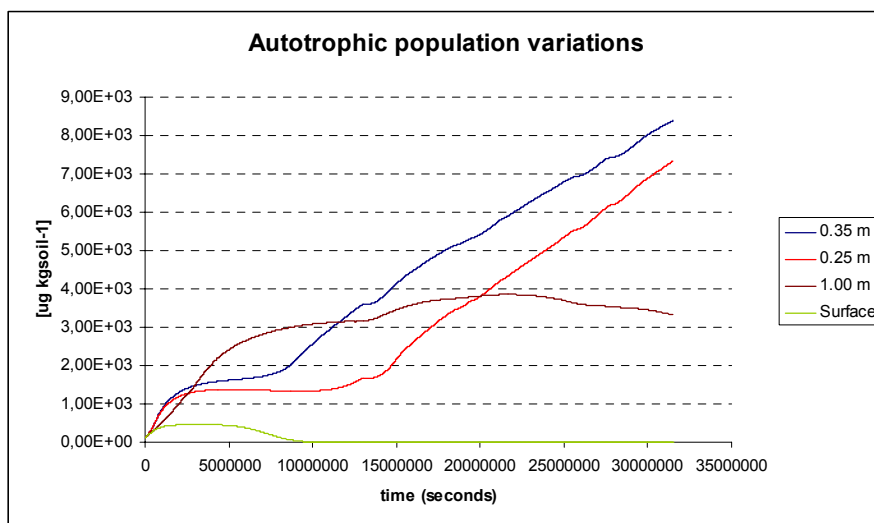


Figure 3.8- Heterotrophic population

This variation of populations with depth explains a usual good agricultural practice that claims that applying organic residues only in the surface will lead higher rates of Nitrate leaching, than distributing them evenly on the first soil centimeters.

If the initial organic matter pools are only applied to the surface, no change will occur on the various properties variation curves for the top layer. On the other hand, no microbial growth will occur for the deeper layers (because there is no substrate). When the Nitrate leaching occurs, there will be no microbial immobilization action in the deeper layers, leading to higher leaching values.

3.2- Why go downhill?

For the second test run, all the conditions from the previous run were repeated with some terrain slope, according to *Figure 3.9*. A sigma vertical coordinate was used, again with 20 vertical layers. For horizontal discretization, an approximately square domain of 5 X 6 cells, each with a square meter.

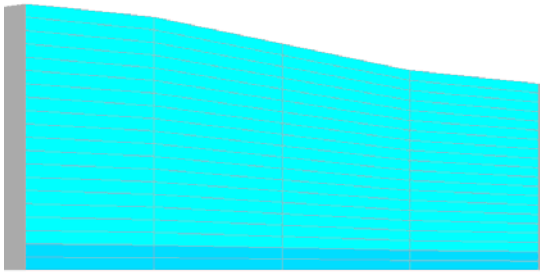


Figure 3.9- Vertical discretization

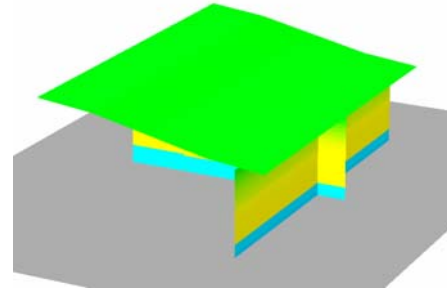


Figure 3.10- Three-dimensional view of the calculus domain.

The first situation worthy to note is that for several time instants water flows according to the gravitational potential *Figure 3.12*- Water velocity vectors, and water content in a normalized scale, at 23 h of 2001/5/24. Even though this seems harmless, the reasons for such a flow are deeper than one may think.

Gravitational potential plays a minor role in water flow (*APPENDIX I*). Small variations in water content can lead to tremendous variations of the soil's matric potential, quickly overriding potential differences due to gravity.

Since water is entering the domain in a uniform fashion, and all the cells have an equal surface, the lower terrain will become damp faster than the upper terrain (greater volume), which should lead to an ascending water flow. However, for some periods, this does not happen. When drying periods occur, or even after short pulses of rain, the lower terrain will dry sooner, by passing the water to the lower layers or by means of evaporation. On the other hand, the upper terrain tends to retain water for long due to its larger volume, and a potential gradient is created forcing water to go "down-hill".

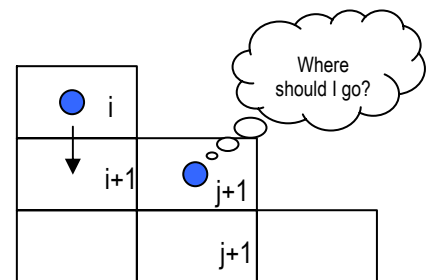


Figure 3.11- Vertical discretization

In Cartesian vertical coordinates, (*Figure 3.11*) both these situations are easier to visualize. If we imagine a single drop of water applied to the entire domain, the water drop at the top of the first cell (i), it must infiltrate to the second one ($i+1$) (no other choice). Once it gets there, it must "decide" where to go next, it can either go to the cell on the right or to the lower cell. Meanwhile the same has happened on the cell (j) and ($j+1$), except in this case the water drop at (j) has more directions to choose from. Repeating this process and regardless of what that choice was, when the first water gets to ($i+1$), ($j+1$) will be drier since

part of the water drop has flown elsewhere, so the water drop at (i+1) will have some matric gradient pulling it to (j+1).

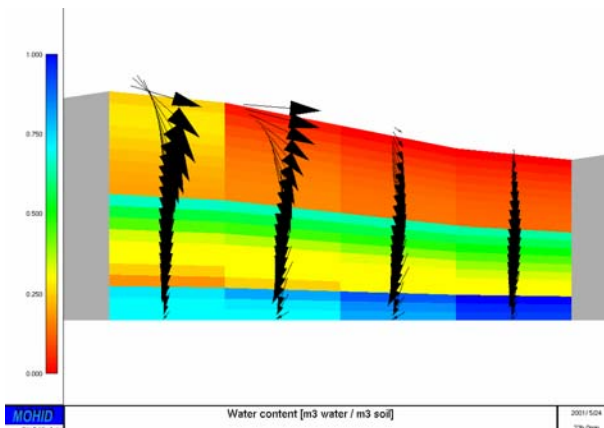


Figure 3.12- Water velocity vectors, and water content in a normalized scale, at 23 h of 2001/5/24

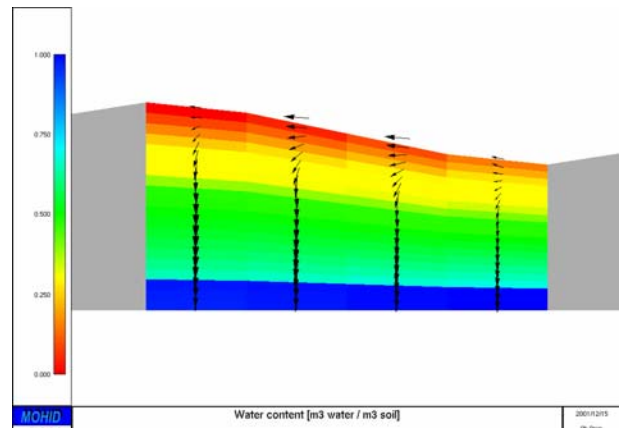


Figure 3.13- Water velocity vectors, and water content in a normalized scale, at 23 h of 2001/12/15

On the other hand if two water drops enter the terrain one after the other, the column of (j) cells would become saturated, while the column of (i) would still have one cell with no water, thus water flow from (j) to (i) would occur).

Sigma vertical coordinates are of some help in these situations since they will help to diminish numerical dispersion, avoiding situations where water fluxes must run trough more cells to diminish the potential gradients



Figure 3.14- Comparison of sigma coordinates and Cartesian ones. In the Cartesian discretization, in order for water to run from the higher potential (i), to the lower (k), it must pass through a cell of intermediate matric potential (j), causing numerical dispersion.

In conclusion, if horizontal fluxes of soil water occur, fluxes for the cycle elements must also occur, but how important are they? Mass transfers from half of the soil column to the other side, were integrated over the run.

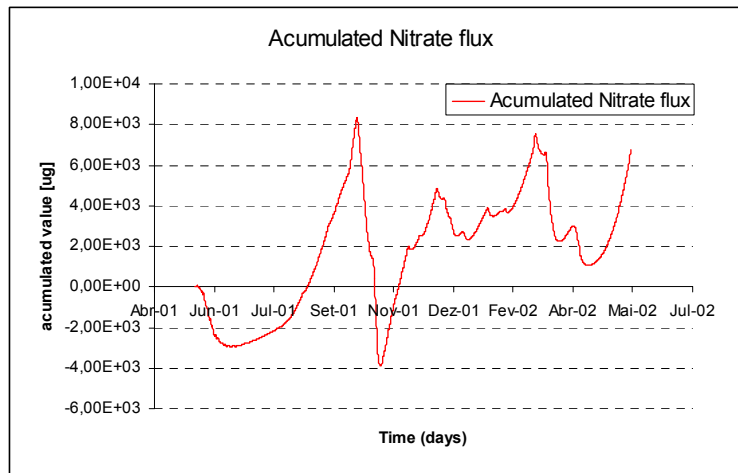


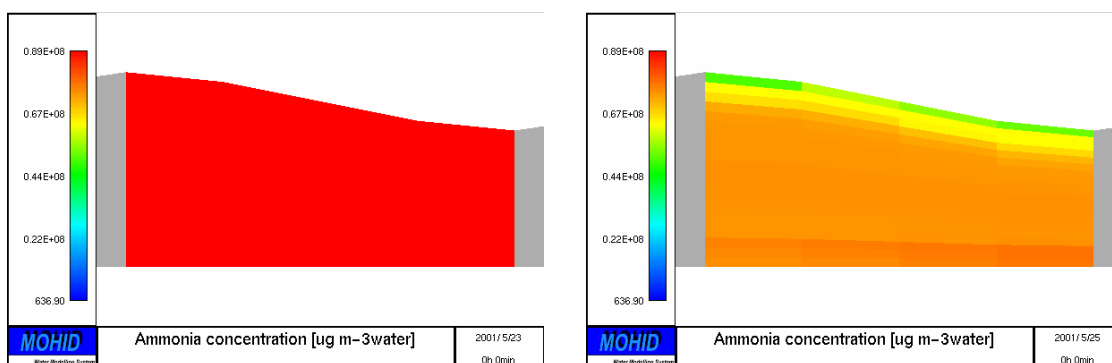
Figure 3.15 - Horizontal mass fluxes

Negative mass values means that the flux has occurred “down- hill”, while Positive values count for ascending mass fluxes.

From the analysis of *Figure 3.15 - Horizontal mass fluxes* have a positive net value for “uphill” fluxes. However when compared to the nitrate mass contained in each of the half domains through which these mass fluxes where accounted (around $1E9 \mu g$), these fluxes can be considered small.

For nitrogen cycling, detailed analysis as those presented in the previous chapter are harder to realize since different depth profiles are obtained for each cell. As so global analysis using MOHID-GUI⁴ are more useful in this situation.

As can be seen from figure cc to cc, the initial ammonia ammonium variations happens in a similar way to *3.1-Simple soil column*



⁴ Graphic User Interface

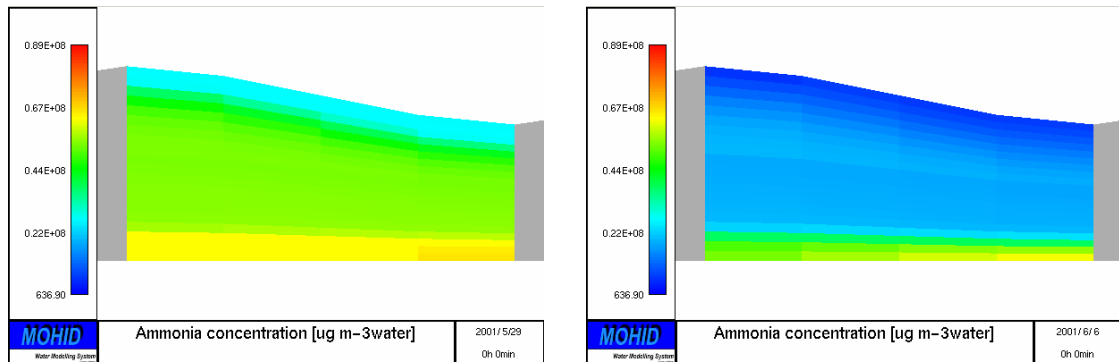


Figure 3.16- Ammonium values at the initial time periods

However, the different water regimes lead to different heterotrophic population distributions

Nitrate levels reach maximum values for different time intervals, residues applications should consider these variations.

3.3- Don't be depressed

Both these simulations were repeated with higher CN ratios for the organic labile residues pool. An initial CN ratio of 50 was established.

Integrating the leached ammonia and nitrate to the lower layer, Figure 3.17 is obtained.

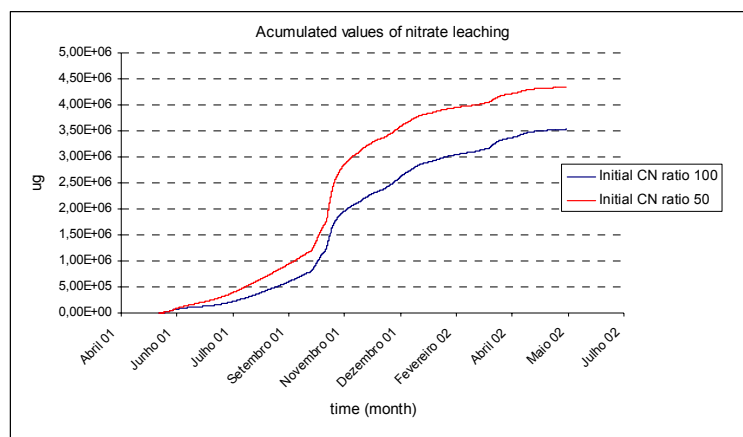


Figure 3.17- Accumulated leached Nitrate mass for a sloped terrain

Note that when the winter rains arrive, the autotrophic microorganisms are at full nitrification rate thus producing higher nitrate leaching rates. An increase of 18% of leached nitrate occurs for a nitrogen input increases of 100%. The leached values are close to those presented by Cameira, 1998 here 30 kg of $NO_3^- - N$ per acre are predicted to leach.

3.4- Cover it up

For the final test run, part of the top cells were covered with a layer with extremely low conductivity. Even though the populations distributions are somewhat different, a smaller area for water to enter did not drastically change the leached nitrate values.

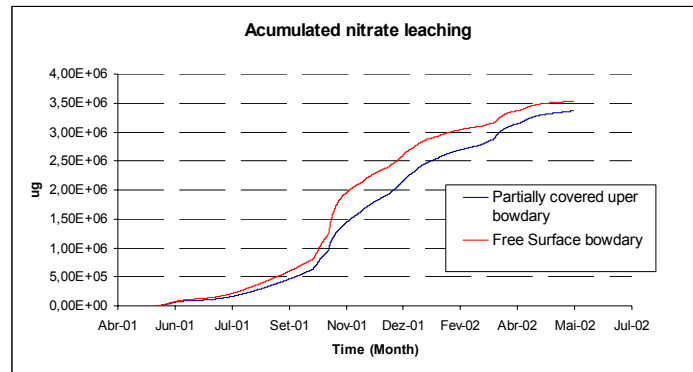


Figure 3.18- Nitrate leaching with 50% of the top area covered

This time only a small difference of 5% less nitrogen was leached.

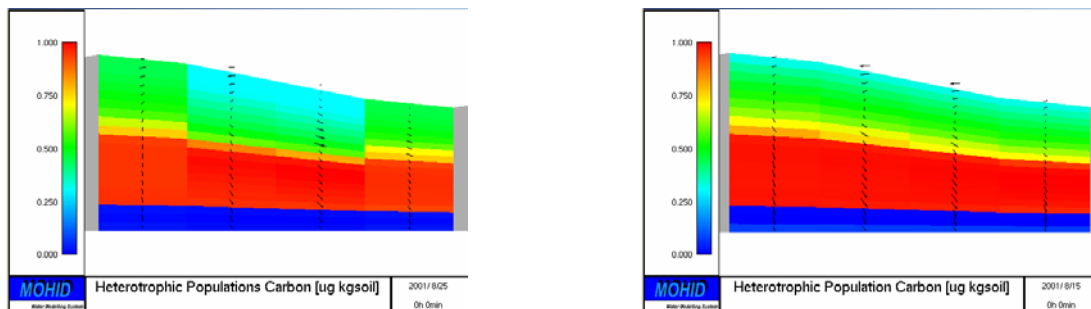


Figure 3.19 - Comparison of Heterotrophic populations distributions (the scales are in normalized values) on the left, the surface is covered.

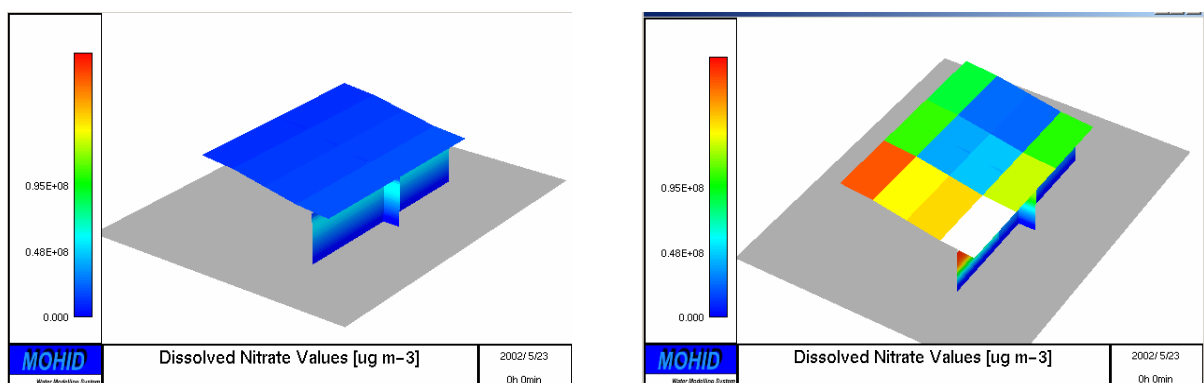


Figure 3.20 - Comparison of Nitrate levels at the end of the run. On the right hand side, the cells where the water was added are the ones with the lower concentration. On the left the whole surface was watered.

4.1- Conclusion / Future work

Water flow and solute transport in unsaturated soil poses an interesting challenge for computational methods. Unlike water flow in streams or oceans, horizontal mixing is very limited, leading to large horizontal heterogeneity and consequent gradients.

In addition, a complex biological structure interacts with soil water and available nutrients creating spatial gradients that horizontal fluxes are not enough to eliminate.

This, and the limited computational capabilities that existed when most soil water flow models were created, were the factor that lead to one-dimensional models. This work attempted to demonstrate that simple terrain variations are enough to invalidate, vertical profiles draw in a single point.

When developing this model, attention was paid on reducing to the maximum the needs for data entrances. Future implementations should include a similar mechanism to RZWQM, which allows the user to run the model from a standard initial conditions simulating several years of selected cultural practices, which means that the model can initialize it self.

Nutrient and environmental conditions have proven to cause temporal variability in Nitrogen dynamics affecting the microbial populations, thus the choice for a more complicated nutrient cycle that explicitly simulates microbial interactions was successful. The control of nitrogen depression periods in different parts of the terrain is the key to good nitrate management and environmental gains. Another interesting conclusion is that in soil, Nitrogen is the problem that one must follow, but when this problem appears when carbon is the limiting nutrient, thus nitrogen modeling in soil must include parallel carbon cycle modeling.

A new structure was tried to implement in the new MOHID module SEDIMENTQUALITY, this has the aim of producing a generic module that could solve any zero dimensional process. Hopefully, in the future creating properties dynamics in an fully three-dimensional model as MOHID will be as easy as “drawing” in a computer interface the state properties and relations between them.

For the present, a reasonable tool was developed in which microbial activity has the possibility of integrating soil air and temperature responses and chemical interactions. Field data validation for such a tool is the challenge that must be faced next. At this point, the models runs for realistic values responding

accordingly to expected, (leached values of Nitrate are in the same order as those presented in Cameira, 1998) but the ultimate test for any model has to be field data validation.

Implemented soil carbon pools are very simple when compared to other models. This leads to a very flexible model where no restraints are placed on the way residues CN ratios vary, however this may not be a realistic simulation. Predatory food-web sensibility analysis should also be performed.

Zymogenous and Autochthonous biomass pool divisions would also make a good addition to the model, allowing long periods of carbon depression to be modeled without having to explicitly stop death rates.

When simple surface water flow, and plant roots are implemented MOHID will be able fully simulate water and nutrient flow for a diversity of terrain morphologies and cultural practices for a diversity of scales.

Bibliographic References

- Alexander, M.; 1961
Introduction to soil microbiology.
John Wiley New York (US)
- Anderson J. D. , 1995
Computational Fluid Dynamics.
McGraw-Hill International editions
- B. Mary, N. Beaudoin, E. Justes & J. M. Machet. 1999
Calculation of nitrogen mineralization and leaching in fallow soil using a simple dynamic model 549- X .
European Journal of Soil Science 50 -42 Volume 49, Issue 4, December 1998
- Bear, J., 1991.
Introduction to Modeling transport Phenomena in Porous Media.
Kluwer academic Publishers
- Bear, J.; Bachmat, Y.; 1972.
Dynamics of fluids in porous Media.
Elsevier, New York
- Brady, N. C.; Wel, R. – 2002
The nature and properties of soils
Prentice Hall, New Jersey
- Broder, M.W. and Wagner. 1988
Microbial colonization and decomposition of corn, wheat, and soybean residue.
Soil Sci. Soc. Am. J. 52:112-117.
- Cameira, M. R. 1999.
Water and nitrogen balance in irrigated corn in the Sorraia Valley. Discussion of the transfer processes
and application of the model RZWQM98.
Ph.D. thesis. Technical University of Lisbon, Agronomy Institute, Portugal.
- Celia, M.A., and E. T. Bououtas, R. L. Zarba. 1990.
A general mass-conservative numerical solution for the unsaturated flow equation.
Water Resour. Res., 26, 1496.
- CHAE Y. M.; Tabatabai M. A.; 1986.
Mineralization in soils Amended with Organic Wastes
Journal of Environmental Quality 15 – 2
- Chun-Ta Lai; Katul, G.; 2000
The dynamic role of root-water uptake in coupling potential to actual transpiration
Advances in water Resources 23 427 – 439
- Elaine R. Firestone and Stanford B.; 2002
Careful Scientific Writing: A Guide for the Nitpicker, the Novice and the Nervous
- Gabrielle, B. and Kengni, L. (1996)
Analysis and field-evaluation of the CERES models' soil components: nitrogen transfer and
transformations.

Soil Sci. Soc. Am. J., 60:142-149.

Hansen, S., M.J. Shaffer, and H.E. Jensen. 1995.
Developments in modelling nitrogen transformations in soil.
Chapter 3, pp 83-107 in Nitrogen fertilizations and the Environment. Marcel Dekker, Inc.

Hirsch C. 1988
Numerical Computation of Internal and External Flows. Volume 1: Fundamentals of numerical discretization.
John Wiley & Sons Lda

Hutzinger, O.; 1985
The handbook of environmental chemistry. v.1 Part A,D. The natural environment and the biogeochemical cycles. v.2 Part A,C. Reactions and Processes
Springer Verlag, Berlin

Jaynes, D.B., and Millee, J. G. (1999).
Evaluation of RZWQM using field measurements data from Iowa MSEA.
Agronomy Journal. 91, 192-200

Johnsson, H., Bergstrvm,L., Jansson, P-E. & Paustian, K. 1987.
Simulation of nitrogen dynamics and losses in a layered agricultural soil.
Agriculture,Ecosystems & Environment 18:333-356.

Jorgensen S.E.; 1994
Fundamentals of Ecological Modelling
Elsevier New York.

Jury, W.A.; Garner, W.R. & Gardner, H.R. 1991.
Soil Physics.
John Wiley. New York.

Kofler, M. 2000
Definitive Guide to excel VBA
Apress

L Ma, MJ Shaffer, JK Boyd, R Waskom, LR Ahuja, KW Rojas, and C Xu ; 1998
Manure management in an irrigated silage corn field: experiment and modelling
Soil Sci. Soc. Am. J. 62: 1006-1017

Linn, D.M. and J.W. Doran. 1984.
Effect of water filled pore space on carbon dioxide and nitrous oxide production in tilled and non-tilled soils.
Soil Sci. Soc. Am. J. 48:1267-1272.

Liwang Ma, Shaffer M.J., Boyd J. K., Waskom R., Ahuja L. R., Rojas K. W. and XU C. 1998
Manure Management in an irrigated Silage Corn Field: Experiments and Modeling
Soil Sci. Soc. Am. J. 62 : 1006 – 1017

M. C. Gonçalves, F. J. Leij & M. G. Schaap. 2001
Pedotransfer functions for solute transport parameters of Portuguese soils;
European Journal of Soil Science 52 – 4

M. J. Goss, K. R. Howse, D. G. Christian, J. A. Catt & T. J. Pepper. 1998
Nitrate leaching: modifying the loss from mineralized organic matter 649

European Journal of Soil Science 49 -4

M.J. Shaffer, 1995

Fate and transport of Nitrogen, What models Can and cannot do Working Paper No 11

Metcalf and Eddy, 1978.

Wastewater Engineering: Treatment, Disposal, Reuse.

McGraw-Hill, NY, pp. 275-878

Neves R., Chambel-Leitão P., Leitão P.C. (2000)

Modelação numérica da circulação da água no solo. O modelo MOHID.

Pedologia, Oeiras 28: 46-55.

Neves, R. Chambel-Leitão P., Leitão P.C., Fernando, R.M., Cameira, M.R. (2002)

Modelação da infiltração e redistribuição de água num Fluvisso.

1º Congresso Nacional das Ciências do Solo. Aceite para publicação na Revista de Ciências Agrárias. Lisboa.

Neves, R.; Chambel-Leitão, P.; Leitão, P. C. 2000.

Modelação numérica da circulação da água no solo.

Pedologia, Oeiras 28: 46-55.

P. Chambel-Leitão, P. Leitão, M. C. Gonçalves, M.E. Mesquita, P. Galvão & R. Neves

Modelação da dinâmica dos solutos da água de rega no solo.

Article submitted for publication in Revista das Ciências Agrárias

P. Garnier, C. Néel, B. Mary & F. Lafolie. 2001

Evaluation of a nitrogen transport and transformation model in a bare soil European

Journal of Soil Science 52 - 2

Parton W.J.; Schimel, Cole, C.V., and Ojima D. S.

Analysis of factors controlling Soil Organic Matter Levels in Great Plains Grasslands

Pereira J.C.F.; 1999

Mecânica de fluidos Computacional Volume – 1

IST

Quintela, A.; 1998

Hidráulica

Fundação Calouste Gulbenkian

S. Marsili- Libelli, M. Manzini 2000

Adaptative Control For Organic Carbon Dosing in Denitrification

Paper presented at WATERMATEX 2000

Shaffer, M.; K. Rojas; D. Ddecoursey e C. Hebson. 1999.

Nutrient chemistry processes –OMNI,

In: Ahua, L.; K. Rojas; J. Hanson; M. Shaffer e L. Ma.. (eds) RZWQM, Modelling managements effects on water quality and crop production, Water Resources publications, LLC, Colorado USA

Simunek, J. M. Sejna and van Genuchten, 1998

The HYDRUS-1D Software Package for Simulating the One-Dimensional Movement of Water, Heat and Multiple Solutes in Variably Saturated Media.

Tveito A.; Winther, R.; 1998

Introduction to Partial Differential Equations
Springer-Verlag New York

APPENDIX

APPENDIX I - Soil Water flow

1-	WATER RETENTION IN SOIL.....	1
1.1-	SOIL WATER CONTENT	1
1.2-	ENERGY STATE OF WATER IN SOIL	1
2-	FLOW THROUGH SATURATED MEDIA	4
2.1-	POISEULLE'S LAW	4
2.2-	DARCY'S LAW	6
3-	FLOW THROUGH UNSATURATED MEDIA.....	8
3.1-	UNSATURATED HYDRAULIC CONDUCTIVITY.....	9
3.2-	MATRIC POTENTIAL	10
3.3-	WATER CONSERVATION EQUATION	11
3.4-	RICHARDS EQUATION FOR TRANSIENT WATER FLOW.....	14
4-	NUMERICAL SOLUTIONS OF THE WATER FLOW EQUATION	16
4.1-	HYDRUS.....	16
4.2-	MOHID	17
4.3-	MATRIC POTENTIAL CURVE RESOLUTION	25
4.4-	HYDRUS METHOD	27
4.5-	MOHID	29
4.5.1	<i>BEHAVIOUR for saturation situations:</i>	32

1- Water retention in soil

The most important characteristics of the soil water phase are the amount of water in a specified amount of soil and the force with which water is retained. The following text introduces these concepts.

1.1-Soil water content

The water content of soils is expressed in two different units, as the volumetric water content θ_v and the gravimetric water content θ_g . The first is the volume of liquid water per volume of soil and the gravimetric water content is the mass of water per mass of dry soil.

1.2-Energy state of water in soil

The retention and movement of water in soils, its uptake by plants or its loss to the atmosphere are all energy related phenomena. In the case of soil, potential and kinetic energy are important. However many processes involving water in soil and plant systems may be dealt with merely by characterizing potential energy changes; kinetic energy enters into equations only implicitly. Nevertheless, the use of potential energy is restricted to those situations where temperature may be regarded to have a negligible effect upon the process under consideration (Jury et al).

There are numerous forces that act upon water in a soil, with various directions, for instance, the gravitational field pulls water vertically downward, force fields caused by the attraction of solid surfaces for water (adhesion) pull water in various directions. Ions dissolved in water have an attractive force for water and resist attempts to move it and there are capillary forces at stake near an air water interface.

This variety of forces and directions in which they are oriented make the description of force networks in soil very difficult. However, it is possible to calculate the potential energy of a unit quantity of water as a result of forces acting upon it.

Potential energy differences from point to point in isothermal systems will determine the direction of flow, the amount of work available for causing flow, or the amount of work that must be done by an outside force to cause flow. As usual, the concept of potential energy must be defined to a reference or standard state, since there is no absolute energy scale. The standard state is defined to be the state of pure (no solutes), free (no external forces other than gravity) water at reference pressure P_0 , reference temperature T_0 and elevation

Z_0 and is arbitrarily given the value zero (Bolt, 1976). This lead to the total soil water potential at temperature T_0 as:

The amount of useful work per unit of pure water that must be done by means of externally applied forces to transfer reversibly and isothermally an infinitesimal amount of water from the standard state to the soil liquid phase at the point under consideration. [BOLT 1976 as in Jury et al. 1991]

The units of the potential energy depend on whether the amount of pure water mentioned is expressed as a mass, volume or weight. TABLE 1.1 summarizes these units

TABLE 1.1 Systems of Units of Total Soil Water Potential

Units	Symbol	Name	Dimensions	SI Units
Energy/mass	μ_T	Chemical potential	L^2/T^2	J/kg
Energy/volume	ψ_T	Soil water potential	M/LT^2	Pa
Energy/weight	h_T	Soil water potential head	L	m

If we break up the transition from the reference poll to the soil in to a series of reversible and isothermal steps the sum of these steps will be equal to the sum of the potential energy changes corresponding to each of the steps.

As so, the total potential energy was divided in

- **Gravitational Potential ψ_z (z in Head Units)** or the energy per unit quantity of water (mass, volume or weight) required to move an infinitesimal amount of pure, free water from the reference elevation, z_0 to the soil water elevation z_{soil} . The reference elevation is purposely designated at a site in the soil profile below that of the soil so that the *gravitational potential* is always positive
- **Solute potential ψ_s (s in head units)** or the change in energy per unit quantity when we maintain all the characteristics of the reference poll, but add solutes identical in composition to the soil solution at the point of interest.

The remaining components of the water potential energy have been defined somewhat differently by many various authors (see Jury et al 1991), but the soil matrix potential is the most important in common soils.

- **Matric Potential** ψ_m (***h in head units***) or the energy per unit quantity of water, required to transfer an infinitesimal amount of water from a reference pool of soil water at the elevation of the soil to the point of interest in the soil at reference air pressure.

This potential accounts for the capacity of the soil to retain water. For instance, a soil with small pores can hold water more tightly than a larger pore soil, since it has a smaller *matric potential*. Water will adhere to the pore's wall, so a smaller pore will have more "units" of water in contact with the wall since it has less "empty" space.

If, for instance a plant will try to remove water from the tighter soil it will have to supply more energy to remove it, because the water is bounded to the soil by ionic links instead of bounded to other water molecules by hydrogen links.

When we add solutes to the reference water or place the reference water in contact with soil particles water will have less mobility since it would be attracted to the solutes or soil. As so both these interactions will reduce water potential energy.

When we place water in a higher elevation than the reference water (as said previously the reference elevation is always below the soil) the potential energy of water will always increase. Figure 1.1, translates these mechanisms.

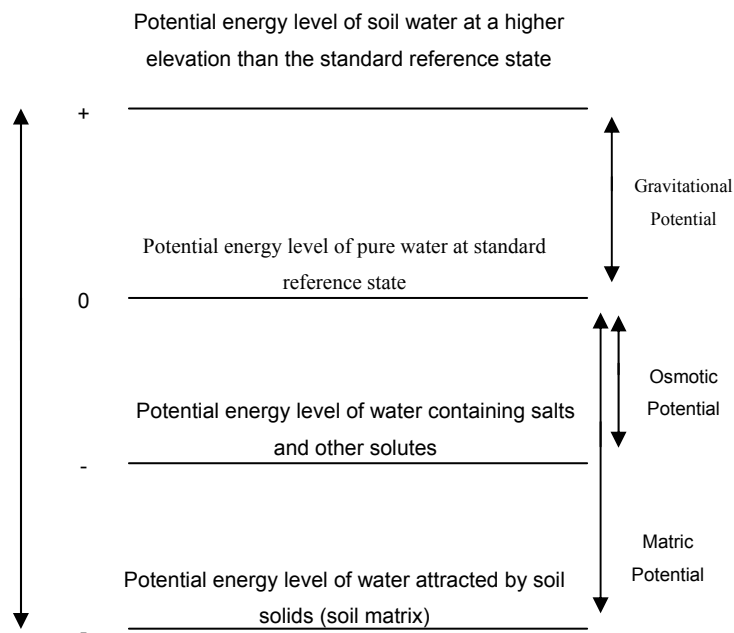


Figure 1.1- Potential energy

2- Flow through saturated media

As said on the previous chapter when two points at different potentials are brought into contact with each other, water will flow from high to low potential in order to restore equilibrium. This rate will depend on the hydraulic resistance of the medium. This chapter introduces how water flow is described in saturated media.

2.1-Poiseuille's Law

The simplest example is the flow through a horizontal capillary tube of diameter D as a result of an imposed hydrostatic pressure difference.

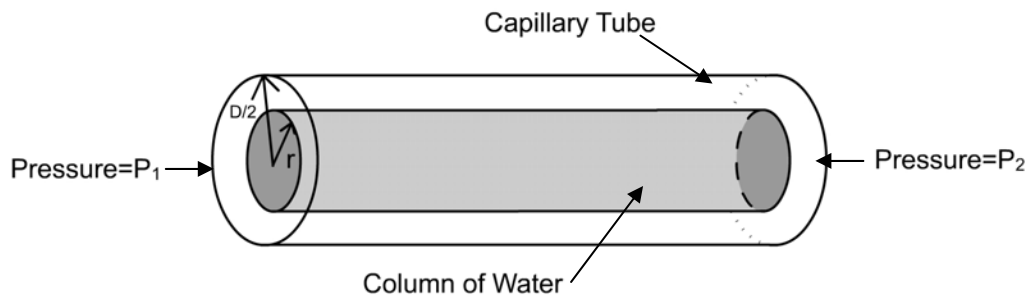


Figure 2.1 Section of a capillary Tube (adapted from Jury et al., 1990)

Since the flow is not accelerating, the net force on any water volume within the tube is equal to zero, and at low flow rates, Newton's law of viscosity (2.1.4) is valid.

The force caused by unequal pressure is:

$$F_p = P_1 \pi r^2 - P_2 \pi r^2 = \Delta P \pi r^2 \quad (2.1.1)$$

The shear force exerted on the water volume by the molecules in contact with the external surface area is:

$$F_s = \tau (2\pi r L) \quad (2.1.2)$$

from (2.1.1) and (2.1.2)

$$\tau = \Delta P r / 2L \quad (2.1.3)$$

Using Newton's law of viscosity (2.1.4) and equating it with (2.1.3) we obtain (2.1.5).

$$\tau = -\mu \frac{dv}{dr} \quad (2.1.4)$$

$$rdr = -\frac{2L\mu}{\Delta P} dv \quad (2.1.5)$$

Considering that the velocity at $r = D/2$ is zero (no slip condition)

$$\int_r^{D/2} rdr = -\frac{2L\mu}{\Delta P} \int_{v(r)}^0 dv \quad (2.1.6)$$

or

$$V(r) = \frac{\Delta P}{4L\mu} \left(\frac{D^2}{4} - r^2 \right) \quad (2.1.7)$$

Poiseuille's law derives from (2.1.7), but represents the volume of water flowing per unit time Q through the capillary. Therefore, we must integrate (2.1.7) over the entire cross-section area of the tube:

$$Q = \iint V(r) dA = \frac{\Delta P}{4L\mu} \int_0^{D/2} \int_0^{2\pi} \left(\frac{D^2}{4} - r^2 \right) r d\phi dr \quad (2.1.8)$$

or finally

$$Q = \frac{\pi D^4}{128\mu} \frac{\Delta P}{L} \quad (2.1.9)$$

Poiseuille's law (2.1.9) is the result of:

- ΔP , which represents the potential energy difference that causes the flow
- $\frac{\pi D^4}{128\mu}$ which can be described as a proportionality coefficient

Since the flow will depend on the fourth power of the tube's diameter, if the diameter drops to half, the flow will need a pressure difference 16 times greater to maintain the same volume of water flowing.

The pressure difference is currently in Pa [$kg\ m^{-1}\ s^{-2}$]. In this case we can regard the pressure difference as a potential energy per unit volume (TABLE 1.1).

If the tube described in Figure 2.1 had some slope, we would have to consider not only the pressure difference, but also the gravitational potential difference of both ends. The same would be valid for kinetic energy differences.

2.2-Darcy's Law

Soil contains a large distribution of pore sizes and channels through which water may flow. The problem is that the exact geometry of these openings is unknown. As so, Newton's law of viscosity cannot be used directly to calculate flow rates in response to water potential gradients. Instead, averages are taken over many pores to obtain macroscopic flow equations that describe water flow through saturated media. Henry Darcy developed this method in 1856 (Quintela, 1998).

If we assume that the soil is rigid, saturated and that no solute membranes exist in the flow path, the total potential energy at any given point can be described as the sum of the hydrostatic pressure and gravitational potential. In head units (TABLE 1.1), this combination is called the hydraulic head H (Jury et al. 1991):

$$H = \frac{P}{\gamma} + z \quad (2.2.1)$$

Where γ accounts for the volumetric weight of water ($\gamma = g \times \rho_w$). Since Pressure corresponds to potential energy per unit volume, $\frac{P}{\gamma}$ is energy per unit weight see (TABLE 1.1).

Expression (2.2.9) was derived using potential energy per unit volume so in order to maintain its validity in head units we must multiply the factor C by γ to turn volume to weight. So expression (2.2.9):

$$Q = \frac{\pi \gamma D^4 \Delta H}{128 \mu L} \quad (2.2.2)$$

or if a flow rate per unit area is considered:

$$J_w = \frac{Q}{\pi r^2} = \frac{\gamma D^2 \Delta H}{32\mu L} \quad (2.2.3)$$

In a saturated¹ soil we can consider an apparent velocity v , or apparent flow rate per unit area J_w through the porous medium in stead of the velocity or unit flow in each of the channels (in this text v_e or J_{we} . So:

$$dQ = J_w dA \quad (2.2.4)$$

Where dA is an elemental area of soil, considering free space and particle filled space. The porosity n_e of the medium can be regarded has ratio between the available area for the flow to take place (not occupied by soil particles) and the total area of the soil.

$$n_e = \frac{A_e}{A} \quad (2.2.5)$$

In a given area of soil the flow can either be described by the apparent unit flow J_w and the total area of soil A , or the unit flow through the open channels J_{we} and their respective area A_e .

$$J_{we} A_e = J_w A \quad (2.2.6)$$

Using (2.2.3), (2.2.5) and (2.2.6)

$$J_w = n_e \frac{\gamma D^2 \Delta H}{32\mu L} \quad (2.2.7)$$

Or,

$$J_w = K_s \frac{\Delta H}{L} \quad (2.2.8)$$

Where K_s is the saturated hydraulic conductivity [LT-1] in head units.

There are several methods to determine the saturated soil's conductivity. The simples is to measure J_w in a laboratory using a vertical column of known length and fitting the experimental data to (2.2.8). This procedure is know as the constant-head method of measuring K_s [Klute and Dirksen, 1986].

¹ A saturated soil has all it's free volume (pores) filled with water

3- Flow through unsaturated media

When soil is not saturated, an air phase as well as the water phase is present. This drastically changes the water flow in the channels described in the previous section.

In unsaturated soil, water is partially bounded by the walls, and partially by an interface with the air phase. The positive water pressure found in saturated soils due to hydrostatic pressure has no meaning in unsaturated soils since the water is in contact with air. The water pressure of the liquid phase is caused by water elevation, attraction to solid surfaces, and the surface tension of the air-water interface. In this case (unsaturated), water pressure is lower than the reference liquid pressure at the same elevation.

Edgar Buckingham in 1907 proposed a modification to *Darcy's law* (2.2.8) to describe flow through unsaturated soil. Considering:

- The driving force for water flow in isothermal, rigid, unsaturated media, containing no solute membranes is the sum of the **matric** and **gravitational** potentials.
- The hydraulic conductivity is a function of the water content or **matric** potential

For vertical flow the *Darcy-Buckingham* flux law is:

$$J_w = -K(h) \frac{\partial H}{\partial z} = -K(h) \frac{\partial}{\partial z} (h + z) \quad (3.1)$$

Equation (3.1) is similar to (2.2.8) but the hydraulic conductivity is a function of h and we are taking in account a very small length of soil, $\lim_{\Delta L \rightarrow 0} \frac{\Delta H}{\Delta L} = \frac{\partial H}{\partial L}$. So (3.1) is written across an infinitesimal thin layer of soil over which $K(h)$ is constant. It may not be written across a finite layer of soil unless special conditions occur (the hydraulic conductivity and matric potential must be uniform).

So, in order to predict water flow in unsaturated soil, the hydraulic conductivity and matric potential must be known. There are several empirical and theoretical models to estimate the hydraulic properties of unsaturated soil $K(h)$ and h . According to (Neves *et al.*, 2000) Mualem (1980) is the most known amongst the theoretical models. The empirical model of Brooks and Corey and the van Genuchten model, were incorporated into several numerical simulation models which allowed them to become standard

models for the hydraulic properties of unsaturated soils. The next section introduces these models, both for matric potential and hydraulic conductivity.

3.1-Unsaturated Hydraulic conductivity

The unsaturated hydraulic conductivity is a nonlinear function of *matric potential* h , or water content θ . There are several reasons for this, for instance let us consider K as a function of θ and imagine a saturated soil with large pores such as a sandy soil.

If no water supply is present or is present at an insufficient rate, the soil layer will drain water until it isn't saturated. At this point the conductivity is not affected, because there are many pores with sufficient water to drain, without having to part it from the pore walls, were water is held more tightly.

As water keeps draining the remaining water has more difficult to drain and the hydraulic conductivity drops. Water will drain from the larger pores and then from tighter ones, so the remaining water will suffer a nonlinear decrease of K , add to this the irregularity of pores shapes and sizes, and we can imagine that the hydraulic conductivity as a non linear function.

The same judgment would be valid for a fine textured (clayey) soil, but in this case water will have much more difficulty do drain even at saturation (2.2.7). Water content will drop much slower when *matric potential* head or water content drop, because there are still many pores that remain unaltered.

There will be a point when the clay soil will even have a higher conductivity then the sandy soil, because at the same *matric potential*, the sandy soil is almost dry while the clay soil still has some water. **Figure 3.1** illustrates this.

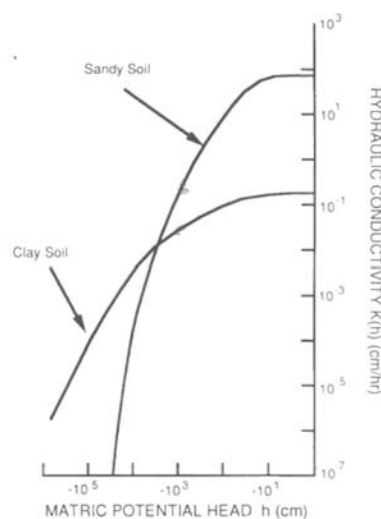


Figure 3.1- Typical hydraulic conductivity curves

There are several analytical models for de unsaturated conductivity, but they all consider the saturated conductivity.

According to (Brooks and Corey, 1964 in Genuchten *et al.*, 1998):

$$K = K_s Se^{2/n+1+2} \quad (3.1.1)$$

where

$$Se = \frac{\theta - \theta_r}{\theta_s - \theta_r} \quad (3.1.2)$$

in which θ_r and θ_s denote the residual and saturated water content, n is a pore size distribution index and l is a pore-connecting parameter assumed to be 2.0 in the original study of *Brooks and Corey* [1964]. We can consider n and l to be empirical coefficients affecting the shape of the hydraulic function.

The most used function for the hydraulic conductivity, was implemented by *van Genuchten* [1980], who used the statistical pore distribution of *Mualem* [1976], to obtain a predictive equation for the unsaturated hydraulic conductivity.

$$K(h) = K_s S_e^l \left[1 - \left(1 - S_e^{1/m} \right)^m \right]^2 \quad (3.1.3)$$

where

$$m = 1 - 1/n, \quad n > 1 \quad (3.1.4)$$

The pore connectivity parameter was estimated [*Mualem*, 1976] to be about 0,5 as an average for many soils

3.2-Matric Potential

The matric Potential h in head units accounts for the potential energy with which water is held by soil particles. Once again this is a highly non linear function of water content.

The matric potential varies very quickly near saturation or near dryness but presents a smooth slope for average values (**Figure 3.2**).

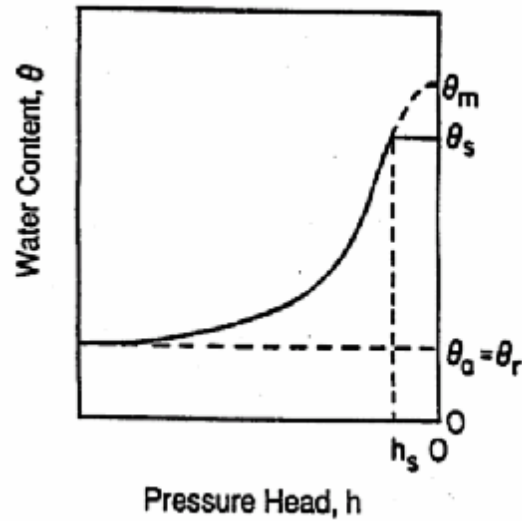


Figure 3.2- Typical $h(\theta)$ curve.

These properties of matric present a problem for numerical models, since large gradients usually cause numerical instability. The way numerical models handle these problems will be addressed in **Section 4-**

The empirical models developed for de $h(\theta)$ by the same authors that developed the conductivity models of **Section 3.1-** however once again the van Genuchten model as the most importance for this study

The van Gnutchten model (Genuchten *et al.*, 1998) is:

$$\theta(h) = \begin{cases} \theta_r + \frac{\theta_s - \theta_r}{[1 + |\alpha h|^n]^m} & h < 0 \\ \theta_s & h \geq 0 \end{cases} \quad (3.2.1)$$

3.3-Water conservation equation

If water fluxes in soil can be calculated, in order to model the water distribution in a given soil, we need to obtain a water mass balance equation.

When we define our control volume or finite element of soil, to which apply the mass conservation principle, we can define it has having well defined infinitesimal volume or a finite control volume. We can also assume that our control volume either is fixed in space (obtaining the equation in conservative form) or moving along

with the flow (non-conservative form). However, with some mathematical manipulation all equations are the same.

In this example we will use the finite control volume fixed in space.

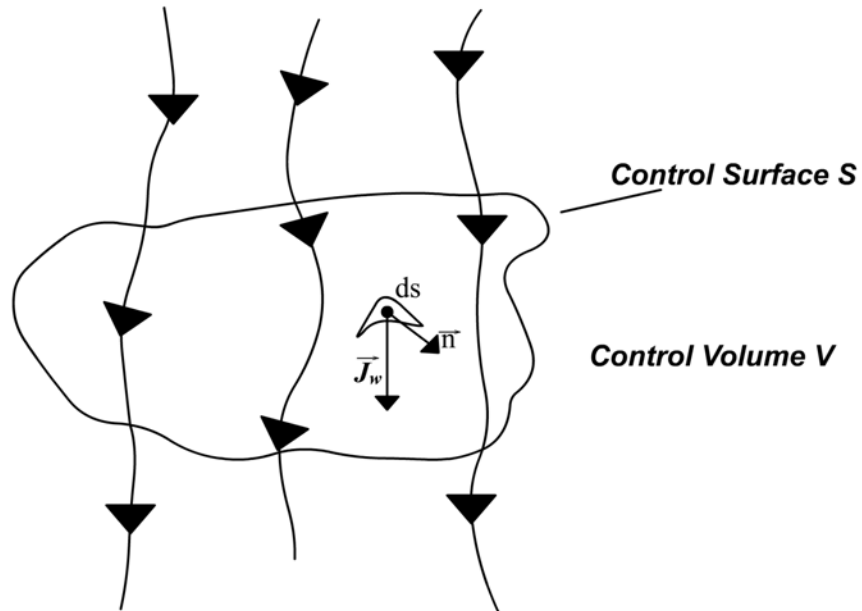


Figure 3.3- **Finite control volume fixed in space**

The water conservation equation can be described as follows:

<p>Decrease of water volume stored in soil during $\Delta t =$</p> <p>-Volume of water entering soil volume during $\Delta t +$</p> <p>Volume of water leaving soil volume during $\Delta t +$</p> <p>Volume of water that as disappeared during Δt by plant root uptake</p>
--

Considering the arbitrary control volume of soil **Figure 3.3**, water moves through the control volume, flowing across the control surface. At a point of the control surface, the flow rate per unit area is J_w the elemental surface area where the flow rate acts is ds and \vec{n} is a unit vector perpendicular to the surface at ds .

The volume flow across the control surface will represent the balance between the volume of water entering the soil's control volume and leaving. The water flow can be represented as the (flow per unit area perpendicular to the control surface) \times (control surface), or

$$J_w \bullet \vec{n} ds \quad (3.3.1)$$

The flow per unit area perpendicular to the control surface is $J_w \bullet \vec{n}$, and since \vec{n} always points out of the control volume the perpendicular flow will be positive for an outflow and negative for an inflow. If we summarize this net volume flow over the whole control volume surface S of **Figure 3.3**, we will obtain the water volume balance, that is:

$$\iint_S J_w \bullet \vec{n} ds \quad (3.3.2)$$

On the other hand the water volume contained in an elemental volume dV of soil is:

$$\iiint_V \theta dV \quad (3.3.3)$$

Considering that θ is the volumetric water content.

The time rate of increase of mass inside V for an infinitesimal Δt is then:

$$\frac{\partial}{\partial t} \iiint_V \theta dV \quad (3.3.4)$$

In turn the time rate of decrease is

$$-\frac{\partial}{\partial t} \iiint_V \theta dV \quad (3.3.5)$$

We can also consider that the water uptake by plant roots as the value r_w and is constant at an infinitesimal small part of our control volume. Summarizing over the whole volume:

$$\iiint_V r_w dV \quad (3.3.6)$$

Combining (3.3.6), (3.3.5) and (3.3.4):

$$\frac{\partial}{\partial t} \iiint_V \theta dV = -\iint_S J_w \bullet \vec{n} ds + \iiint_V r_w dV \quad (3.3.7)$$

Since the control volume used in the derivation of (3.3.5) is fixed in space, it doesn't change in time, and hence the time derivative $\partial/\partial t$ can be placed inside the integral.

$$\iiint_V \frac{\partial}{\partial t} \theta \, dV \quad (3.3.8)$$

Using the divergence theorem the right hand side of (3.3.5) becomes:

$$\iint_S J_w \cdot \bar{n} \, ds = \iiint_V \nabla \cdot J_w \, dV \quad (3.3.9)$$

Using (3.3.7), (3.3.6) in (3.3.5) we have:

$$\iiint_V \left[\frac{\partial \theta}{\partial t} + \nabla \cdot J_w - r_w \right] dV = 0 \quad (3.3.10)$$

or:

$$\frac{\partial \theta}{\partial t} = -\nabla \cdot J_w + r_w \quad (3.3.11)$$

Equation (3.3.5) is the integral form of the water conservation equation while (3.3.11) is the partial differential equation of the continuity equation. Equation (3.3.11) could have been obtained directly from the mass balance of an infinitesimal small element fixed in space. Never less, both of them are in the conservative form.

3.4-Richards Equation for transient Water Flow

Combining the expression (3.3.11) with the *Buckingham-Darcy* flux equation (3.1), we can derive Richards equation (3.4.1) (Jury et al.), that predicts the water content or matric potential in a soil during transient flow.

$$\frac{\partial \theta}{\partial t} = \nabla \cdot [K(h) \nabla H] \quad (3.4.1)$$

Where $H = h + z$.

Considering that there is only vertical flow and no plant roots are present ($r_w = 0$), Richards equation is:

$$\frac{\partial \theta}{\partial t} = \frac{\partial}{\partial z} \left[K(h) \frac{\partial (H)}{\partial z} \right] \quad (3.4.2)$$

Equation (3.4.1) or (3.4.2), can't be solved in the formed their in since there hare 2 unknowns h and θ . This can be overcome by using the water characteristic retention function that expresses h as a function of θ . Using the chain rule of differentiation and considering that :

$$C(h) = \frac{d\theta}{dh} \quad (3.4.3)$$

$$D(\theta) = K(\theta) \frac{\partial h}{\partial \theta} \quad (3.4.4)$$

Equation (3.4.1) can be expressed in three different forms:

$$C(h) \frac{\partial h}{\partial t} - \nabla \cdot (K(h) \nabla h) - \frac{\partial K(h)}{\partial z} = 0 \quad (3.4.5)$$

$$\frac{\partial \theta}{\partial t} - \nabla \cdot (D(\theta) \nabla \theta) - \frac{\partial K(\theta)}{\partial z} = 0 \quad (3.4.6)$$

$$\frac{\partial \theta}{\partial t} - \nabla \cdot (K(h) \nabla h) - \frac{\partial K(h)}{\partial z} = 0 \quad (3.4.7)$$

(3.4.5) is the *matric potential* form of Richards Equation. The water content of the soil was considered as a function of *matric potential* $\theta(h)$.

(3.4.6) is the water content form of the Richards Equation, the *matric potential* was considered a function of water content, so $K(h) = K(\theta)$ and:

$$\nabla h(\theta) = \frac{\partial h}{\partial \theta} \nabla \theta \quad (3.4.8)$$

(3.4.7) is the same has (3.4.1), but with $H = h + z$. It's the mixed form of the Richards Equation

According to (Celia *et al.*, 1990), the discrete approximations to the θ based equation, such as finite elements or finite differences, can be formulated so that they are perfectly mass conservative. However this

form of the Richard's equation degenerates in fully saturated media, and because material discontinuities produce discontinuous θ profiles, this equation is usually not used for general groundwater hydrology problems.

The same author (Celia *et al.*, 1990) concluded that the discrete approximations to the h based equation displayed poor mass balance and associated poor accuracy. In conclusion it seems that the mixed equation combines benefits from the other forms, circumventing major problems such as poor accuracy (h form) and restricted applicability (θ form).

Numerical solutions to the mixed Richard's equation will be discussed in the next chapter.

4- Numerical solutions of the water flow equation

There are several models that simulate water flow in unsaturated media (e.g. Hydrus, Modflow, Macro), most of them developed for specific applications.

The **HYDRUS** model was developed the US SALYNITY LABORATORY, AGRICULTURAL RESEACH SERVICE, and numerically solves the Richard's mixed equation for variably saturated water flow and convective-dispersion type equations for heat and solute transport. It enjoys large acceptance in the scientific community, due to the large amount of publications that support software.

On the other hand MOHID was initially developed to simulate the bi-dimensional flow of tides in costal areas (Neves, 1985). The program was successively enlarged to simulate Boussinesq waves (Silva, 1992), water quality (Portela, 1996) and three-dimensional flows. This model is divided into modules, each of which as its on function. Later, more modules where developed to allow the simulation of water flow in damns.

The following analysis is centered on these too models, since the first can be regarded a standard and this work uses the second.

4.1-HYDRUS

HYDRUS uses a finite difference approach to Richard's equation and incorporates convection-diffusion type equations for heat and solute transport.

Several curves are available to evaluate the unsaturated soil hydraulic Properties, (Brooks and corey, 1964; van Gnuchten 1980; and Vogel and Císlerová, 1988). Soil hydraulic functions dependence of temperature is also implemented.

Hysteresis (different pressure head for the same water content for wetting and drying episodes) is incorporated by using the empirical model developed by Scott et al. 1983.

4.2-MOHID

The soil module that describes water flow in unsaturated media was incorporated in MOHID, reusing modules that were already implemented. Chapter 2.5-FORTRAN *implementation*, briefly resumes how MODULESOIL interacts with other modules.

MOHID uses a finite volume discretization and allows different vertical discretization (sigma, Cartesian).

The ADI method (Peaceman and Rachford 1955, as in J.C.F. Pereira, 1999) for time discretization is used. This approach has been used in all the versions of the hydrodynamic model in MOHID (Neves 1985, Santos 1995, Martins 2000). As so, the time step Δt will be divided into 3 time levels. In each of these time steps, Richard's equation will be solved implicitly in one direction and explicitly on the too remaining directions *Figure 4.1- The ADI method, adapted from Anderson (1995)* demonstrates this method for a bi-dimensional situation.

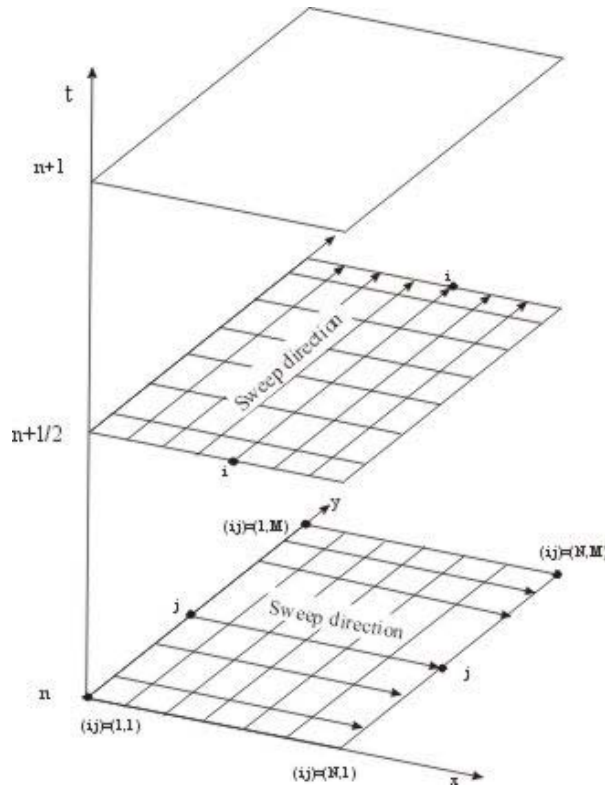


Figure 4.1- The ADI method, adapted from Anderson (1995)

Since two directions are present, the time step is fractioned into two sub-time steps. For the first semi interval, the equation is solved explicitly in the (i) direction and implicitly in the (j) direction, producing a “j sweep”, the obtained values are then applied to a situation where (i) is solved in an implicit fashion and (j) in an explicit manner, obtaining the final values at the final time level.

This will prevent solving a system matrix that may not be diagonally dominant, since for each of the “sub-time” steps a triagonal matrix will be present.

For instance, let us consider the finite volume in **Figure 4.2**.

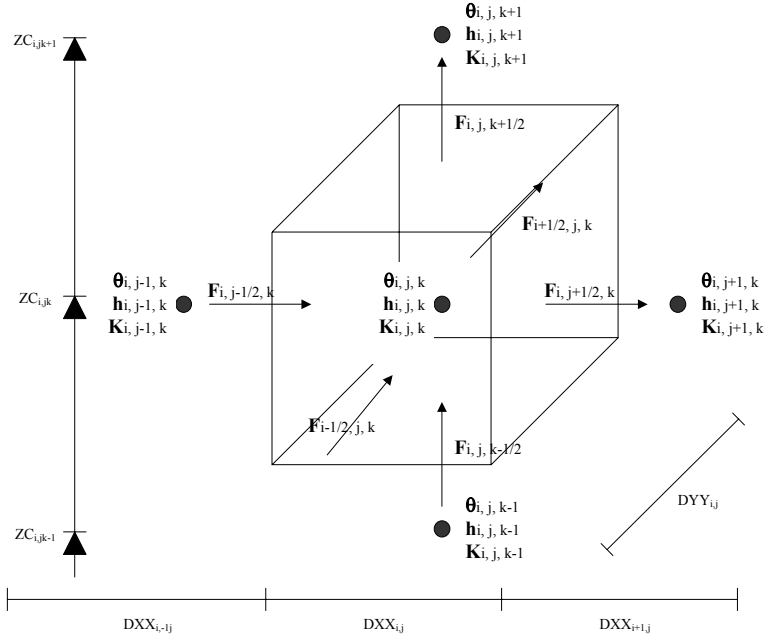


Figure 4.2- Finite volume

The fluxes are represented by F and the remaining symbols have the meaning that as defined previously.

If we consider the usual implicit approach for this problem (Crank Nicholson for instance) in a bi-dimensional flow (we won't consider flow in the j direction) in K and I , we would obtain

$$\frac{\partial \theta}{\partial t} = -\frac{\partial J_w}{\partial x} - \frac{\partial J_w}{\partial z} \quad (4.2.1)$$

$$\frac{\theta_{i,j}^{n+1} - \theta_{i,j}^n}{\Delta t} = - \left(\frac{1}{2} \frac{J_{i+1/2}^n - J_{i-1/2}^n}{\Delta x} + \frac{1}{2} \frac{J_{i+1/2}^{n+1} - J_{i-1/2}^{n+1}}{\Delta x} + \frac{1}{2} \frac{J_{K+1/2}^n - J_{K-1/2}^n}{\Delta Z} + \frac{1}{2} \frac{J_{K+1/2}^{n+1} - J_{K-1/2}^{n+1}}{\Delta z} \right) \quad (4.2.2)$$

Rearranging, and considering that we can relate the fluxes with the water content (see 3-):

$$a\theta_{i-1}^{n+1} + b\theta_{K-1}^{n+1} + c\theta_{i,K}^{n+1} + d\theta_{i+1}^{n+1} + e\theta_{K+1}^{n+1} = d^n \quad (4.2.3)$$

When solving for the hole control volume we would obtain a system with 5 diagonal lines in the coefficient matrix, relative to the top cell, bottom cell, east and west cells.

$$\theta_{i,j,k}^{n+1} - \frac{\Delta t}{V_{i,j,k}^{n+1}} (-F_{i,j,K+1/2}^{n+1} + F_{i,j,K-1/2}^{n+1}) = \frac{V_{i,j,k}^n}{V_{i,j,k}^{n+1}} \theta_{i,j,k}^n + \frac{\Delta t}{V_{i,j,k}^{n+1}} (-F_{i+1/2,j,k}^n + F_{i-1/2,j,k}^n - F_{i,j+1/2,k}^n + F_{i,j-1/2,k}^n) \quad (4.2.7)$$

The terms on the right side of the equation are known quantities, considering that we can predict the volume changes of the control element, and will be referred to as *Ticoef* and according to **Figure 4.2**, and the Darcy-Buckingham equation (3.1).

$$J_{i+1/2,j,k}^n = -K(\theta_{i+1/2,j,k}^n) \left[\frac{h_{i+1,j,k}^n - h_{i,j,k}^n}{\frac{DYY_{i+1,j} - DYY_{i,j}}{2}} \right]$$

$$J_{i-1/2,j,k}^n = -K(\theta_{i-1/2,j,k}^n) \left[\frac{h_{i,j,k}^n - h_{i-1,j,k}^n}{\frac{DYY_{i,j} - DYY_{i-1,j}}{2}} \right]$$

$$J_{i,j+1/2,k}^n = -K(\theta_{i,j+1/2,k}^n) \left[\frac{h_{i,j+1,k}^n - h_{i,j,k}^n}{\frac{DXX_{i+1,j} - DXX_{i,j}}{2}} \right]$$

$$J_{i,j-1/2,k}^n = -K(\theta_{i,j-1/2,k}^n) \left[\frac{h_{i,j,k}^n - h_{i,j-1,k}^n}{\frac{DXX_{i,j} - DXX_{i-1,j}}{2}} \right]$$

Where the pressure head term was described via central differences.

The flux F on each face will be $F = AJ_w$ where A the area of the face where the flux occurs is.

So:

$$\begin{aligned}
Ticoef = & \frac{V_{i,j,k}^n}{V_{i,j,k}^{n+1}} \theta_{ijk}^n \\
& + \frac{\Delta t}{V_{i,j,k}^{n+1}} \left(A_{i,j+1/2,k}^n K(\theta_{i,j+1/2,k}^n) \left[\frac{h_{i,j+1/2,k}^n - h_{i,j,k}^n}{(DXX_{i+1j} + DXX_{ij})} \right] - A_{i,j-1/2,k}^n K(\theta_{i,j-1/2,k}^n) \left[\frac{h_{i,j,k}^n - h_{i,j-1k}^n}{(DXX_{ij} + DXX_{i-1j})} \right] \right) \\
& + \frac{\Delta t}{V_{i,j,k}^{n+1}} \left(A_{i+1/2,j,k}^n K(\theta_{i+1/2,j,k}^n) \left[\frac{h_{i+1,j,k}^n - h_{i,j,k}^n}{(DYY_{i+1j} + DYY_{ij})} \right] - A_{i-1/2,j,k}^n K(\theta_{i-1/2,j,k}^n) \left[\frac{h_{ij,k}^n - h_{i-1j,k}^n}{(DYY_{ij} + DYY_{i-1j})} \right] \right)
\end{aligned} \quad (4.2.8)$$

For the terms on the left side of (4.2.7) are the fluxes of water in the new time step. As so, they will depend on the vertically adjacent cells water content according to (4.2.10) and (4.2.10):

$$J_{i,j,k+1/2}^{n+1} = -K(\theta_{i,j,k+1/2}^{n+1}) \left[\frac{h_{i,j,k+1}^{n+1} - h_{i,j,k}^{n+1}}{ZCC_{i,j,k+1} - ZCC_{i,j,k}} + 1 \right] \quad (4.2.9)$$

$$J_{i,j,k-1/2}^{n+1} = -K(\theta_{i,j,k-1/2}^{n+1}) \left[\frac{h_{i,j,k}^{n+1} - h_{i,j,k-1}^{n+1}}{ZCC_{i,j,k} - ZCC_{i,j,k-1}} + 1 \right] \quad (4.2.10)$$

These fluxes cannot be easily evaluated, since eq. (4.2.9) and (4.2.10) are not linear. The conductivity multiplies by the matric potential and both are evaluated in n+1 and are unknown.

The problem that arises in the “implicit direction sweep” can be simplified by evaluating the coefficients (in this case the unsaturated conductivity) using the water content values of the previous step; according to Anderson 1995 this is called “lagging the coefficients”. The same can be said about the matric potential that is not a linear function of θ , except in this case we will obtain a linear system supposing that $h^{n+1} = f(\theta^n)\theta^{n+1}$:

These simplification will work if we have a soft differential equation (where the conductivity and matric potential are not a strong function of the water content). On the other hand, in dry or wet situations (see Figure 3.2- **Typical $h(\theta)$ curve.** and Figure 3.1- **Typical hydraulic conductivity curves**) the lagged coefficients will produce mass balance errors. To overcome this problem an iterative process must be set up, where the new θ are used to correct the lagged coefficients that are once again used to evaluate new θ values, until the θ variations between two consecutive calculations are neglectable. This is usually referred to as an Piccard (or fixed point) iterative process. For

unsaturated soil and using the mixed form Richard equation an faster algorithm than simple fixed point iterations was derived in Celia et al. 1990.

Continuing with the previous derivation:

$$\theta_{i,j,k}^{n+1} - \frac{\Delta t}{V_{i,j,k}^{n+1}} \left(A_{i,j,k+1/2}^{n+1} K(\theta_{i,j,k+1/2}^n) \left[\frac{f(\theta_{i,j,k+1}^n) \theta_{i,j,k+1}^{n+1} - f(\theta_{i,j,k}^n) \theta_{i,j,k}^{n+1}}{ZCC_{i,j,k+1} - ZCC_{i,j,k}} + 1 \right] - A_{i,j,k-1/2}^{n+1} K(\theta_{i,j,k-1/2}^n) \left[\frac{f(\theta_{i,j,k}^n) \theta_{i,j,k}^{n+1} - f(\theta_{i,j,k-1}^n) \theta_{i,j,k-1}^{n+1}}{ZCC_{i,j,k} - ZCC_{i,j,k-1}} + 1 \right] \right) = Ticoef$$

rearranging:

$$\begin{aligned} \theta_{i,j,k}^{n+1} \left[1 - \frac{\Delta t}{V_{i,j,k}^{n+1}} \left(-A_{i,j,k+1/2}^{n+1} K(\theta_{i,j,k+1/2}^{n+1}) \left[\frac{f(\theta_{i,j,k}^n)}{ZCC_{i,j,k+1} - ZCC_{i,j,k}} \right] - A_{i,j,k-1/2}^{n+1} K(\theta_{i,j,k-1/2}^{n+1}) \left[\frac{f(\theta_{i,j,k}^n)}{ZCC_{i,j,k} - ZCC_{i,j,k-1}} \right] \right) \right] \\ + \theta_{i,j,k+1}^{n+1} \left[-\frac{\Delta t}{V_{i,j,k}^{n+1}} A_{i,j,k+1/2}^{n+1} K(\theta_{i,j,k+1/2}^{n+1}) \left[\frac{f(\theta_{i,j,k+1}^n)}{ZCC_{i,j,k+1} - ZCC_{i,j,k}} \right] \right] \\ + \theta_{i,j,k-1}^{n+1} \left[-\frac{\Delta t}{V_{i,j,k}^{n+1}} A_{i,j,k-1/2}^{n+1} K(\theta_{i,j,k-1/2}^{n+1}) \left[\frac{f(\theta_{i,j,k-1}^n)}{ZCC_{i,j,k+1} - ZCC_{i,j,k}} \right] \right] \\ - \frac{\Delta t}{V_{i,j,k}^{n+1}} A_{i,j,k+1/2}^{n+1} K(\theta_{i,j,k+1/2}^n) + \frac{\Delta t}{V_{i,j,k}^{n+1}} A_{i,j,k-1/2}^{n+1} K(\theta_{i,j,k-1/2}^n) = Ticoef \end{aligned}$$

The final term before the equality doesn't multiply by any cell's water content and as so can be sent to *Ticoef*.

Considering that *Ecoef* multiplies by the cell in analysis, *Fcoef* the top cell and *Dcoef* the bottom cell:

$$Ecoef = 1 - \frac{\Delta t}{V_{i,j,k}^{n+1}} \left(\begin{array}{c} -A_{i,j,k+1/2}^{n+1} K(\theta_{i,j,k+1/2}^{n+1}) \left[\frac{f(\theta_{i,j,k}^n)}{ZCC_{i,j,k+1} - ZCC_{i,j,k}} \right] \\ -A_{i,j,k-1/2}^{n+1} K(\theta_{i,j,k-1/2}^{n+1}) \left[\frac{f(\theta_{i,j,k}^n)}{ZCC_{i,j,k} - ZCC_{i,j,k-1}} \right] \end{array} \right)$$

$$Dcoef = -\frac{\Delta t}{V_{i,j,k}^{n+1}} A_{i,j,k-1/2}^{n+1} K(\theta_{i,j,k-1/2}^{n+1}) \left[\frac{f(\theta_{i,j,k-1}^n)}{ZCC_{i,j,k+1} - ZCC_{i,j,k}} \right]$$

$$Fcoef = -\frac{\Delta t}{V_{i,j,k}^{n+1}} A_{i,j,k+1/2}^{n+1} K(\theta_{i,j,k+1/2}^{n+1}) \left[\frac{f(\theta_{i,j,k+1}^n)}{ZCC_{i,j,k+1} - ZCC_{i,j,k}} \right]$$

$$Ticoef = \frac{V_{i,j,k}^n}{V_{i,j,k}^{n+1}} \theta_{ijk}^t$$

$$\begin{aligned} & + \frac{\Delta t}{V_{i,j,k}^{n+1}} \left(\begin{array}{c} A_{i,j+1/2,k}^n K(\theta_{ij+\frac{1}{2}k}^n) \left[\frac{h_{ij+1k}^t - h_{ijk}^t}{(DXX_{i+1j} + DXX_{ij})} \right] - A_{i,j-1/2,k}^n K(\theta_{ij-\frac{1}{2}k}^n) \left[\frac{h_{ijk}^t - h_{ij-1k}^t}{(DXX_{ij} + DXX_{i-1j})} \right] \\ A_{i+1/2,j,k}^n K(\theta_{i+\frac{1}{2}jk}^n) \left[\frac{h_{i+1jk}^t - h_{ijk}^t}{(DYY_{i+1j} + DYY_{ij})} \right] - A_{i-1/2,j,k}^n K(\theta_{i-\frac{1}{2}jk}^n) \left[\frac{h_{ijk}^t - h_{i-1jk}^t}{(DYY_{ij} + DYY_{i-1j})} \right] \end{array} \right) \\ & + \frac{\Delta t}{V_{i,j,k}^{n+1}} A_{i,j,k+1/2}^{n+1} K(\theta_{i,j,k+1/2}^{n+1}) - \frac{\Delta t}{V_{i,j,k}^{n+1}} A_{i,j,k-1/2}^{n+1} K(\theta_{i,j,k-1/2}^{n+1}) \end{aligned}$$

At this point Richard's equation can be described as:

$$Dcoef \theta_{i,j,k-1}^{n+1} + Ecoef \theta_{i,j,k}^{n+1} + Fcoef \theta_{ijk+1}^{n+1} = Ticoef$$

As so, the system will solve a tridiagonal matrix using Thomas Algorithm.

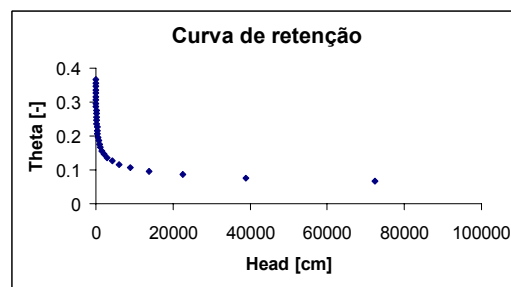
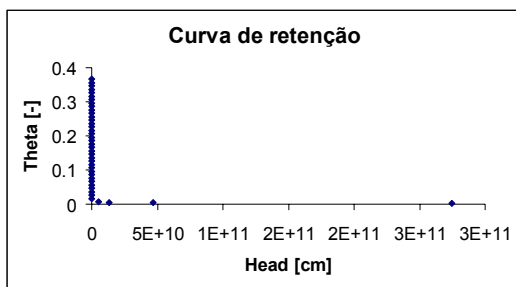
The same procedure can be used in a x and y direction sweep. In each of these sub time steps the resulting system will also be a tridiagonal matrix. After all the different directions are swept, the new water volume concentrations are found.

4.3-Matric potential curve resolution

The main difficulty in solving water flow in unsaturated media is the exponential behavior of the soil water retention curve.

When the matric potential h is very low (near saturation), water content θ suffers great variations for small time steps. On the other hand, if matric potentials are very high, θ will no vary.

An iterative process was implemented to deal with this situation, that allows to increase or diminish the time step, according to the model's convergence. However, for such an iterative process to work, one must establish maximum tolerations for theta variations in a given time step. Due to the exponential behavior of the water retention curve, this variation cannot be the same for every initial water content. A tolerance of θ in the order of 0.001, may be too much near saturation (where small variations of water content can cause massive variations of matric potential), and at the same time be a small variation for small values of θ .



theta as a function of h- Retention curves adapted from a MOHID manual.

tetar	tetas	nfit	mfit	alfa	cons
0.001	0.366	1.2298	0.18686	0.0252	14.5

When θ is close to residual values (θ_r) (dry soil) h values can very high. Its usual for these functions to return physically impossible values of h . van Genuchten considers that the residual water content remains in the soil when a pressure of 15 atmospheres is applied to the soil. Retention functions obtained are a statistical approach to a set of experimental values. Sometimes, θ_r is only reached for values far greater than 15 atmospheres (sometimes millions). From a theoretical point of view only when $d\theta/dh=0$ is reached the residual water content should be defined. Most authors consider that this should only be regarded as a statistical parameter with no physical meaning.

As so, large gradients can occur which lead to massive (sometimes impossible) water fluxes. The next table shows some coupled values of the variation of θ and h . In fact, for water contents between 0.0015 and 0.005 the pressure gradient is around $1.0E+05$.

θ	h
0.036	1070325
0.026	4628166
0.016	42737424
0.006	5.09E+09
0.005	1.35E+10
0.004	4.7E+10
0.003	2.75E+11
0.002	5.61E+12
0.0015	1.14E+14

This problem can be solved if one establishes that before the 15 atmospheres are reached, the pressure should vary linearly until the residual value θ_r is reached.

So how can one determine what is an acceptable water content variation?

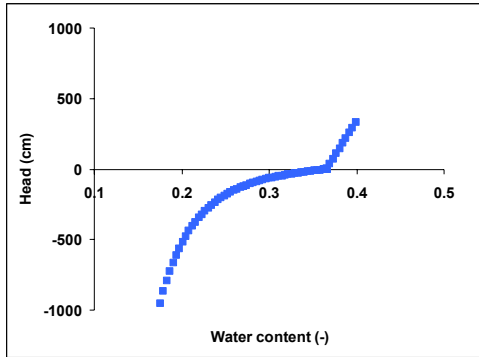
Considering:

- h^{it+1} – Value for the effective pressure in the iteration **it+1**.
- h^{it} – Value for the effective pressure in the iteration **it**.
- θ^{it+1} – Water content in **it+1**.
- θ^{it} – Water content in **it**.
- $\Delta\theta = \theta^{it+1} - \theta^{it}$
- $\frac{\partial h}{\partial \theta}$ - h derivate in order to θ .

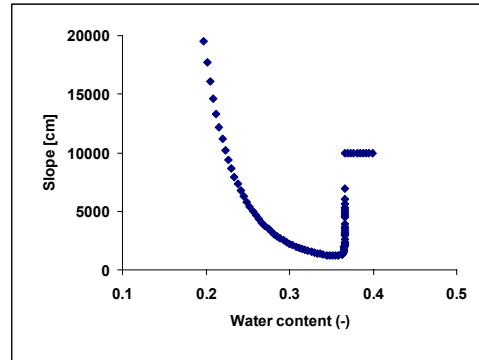
So:

- If $h'(\theta)$ "is high" $\Delta\theta * \frac{\partial h}{\partial \theta} < h_{tol}$
- If $h'(\theta)$ is low $\Delta\theta < \theta_{tol}$

If one decides that a high $h'(\theta)$ is about 3000, this means that h_{tol} will only be used for declines smaller than 3000.



Water retention curve and the pressure curve for values over the saturation point



Decline for the water retention curve and the pressure curve for values over the saturation point

Tetar	Tetas	nfit	mfit	alfa	cons	Ss
0.001	0.366	1.2298	0.18686	0.0252	14.5	1.00E-04

4.4-HYDRUS Method

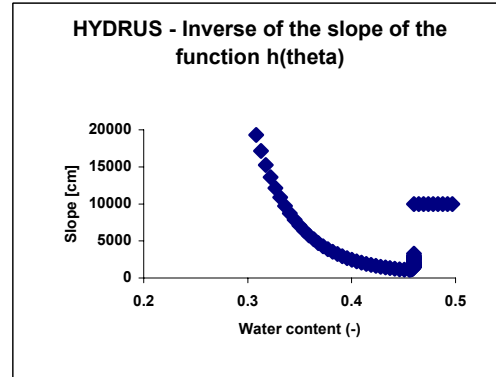
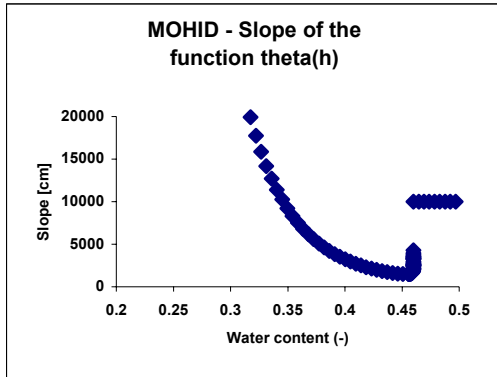
In HYDRUS h varies in time and the values of θ are obtained from h through the water retention saturation curve

$$\theta(h) = \theta_r + \frac{\theta_s - \theta_r}{(1 + |\alpha h|^N)^M}$$

The derived of this function is termed the soil water capacity function, in HYDRUS:

$$\theta'(h) = M * N(\alpha^N) * (-h^{(N-1)}) * (1 + (-\alpha * h)^N)^{-(M-1)} (\theta_s - \theta_r)$$

Comparing the inverse of this function $\theta'(h)$, with the function $h'(\theta)$ used in MOHID one can verify that they behave similarly.



The function $\theta(h)$ is used to calculate the θ difference between two iterations biased on a matric potential variation. h :

$$\Delta\theta = \left| \theta^{it} - \theta^{it} + \frac{\partial\theta}{\partial h^{it}} (h^{it+1} - h^{it}) \frac{1}{\theta_s - \theta_r} \right|$$

If $h^{it} < h_s \wedge h^{it+1} < h_s$

$$\Delta\theta = \left| \theta^{it} - \theta^{it+1} \right| \text{ where } \theta^{it+1} = \theta^{it} + \frac{\partial\theta}{\partial h^{it}} (h^{it+1} - h^{it}) \frac{1}{\theta_s - \theta_r}$$

$$\Delta\theta = \left| \theta^{it} - \theta^{it+1} \right| \Leftrightarrow \Delta\theta = \left| \theta^{it} - \theta^{it} + \frac{\partial\theta}{\partial h^{it}} (h^{it+1} - h^{it}) \frac{1}{\theta_s - \theta_r} \right| \Leftrightarrow$$

$$\Delta\theta = \left| \frac{\partial\theta}{\partial h^{it}} (h^{it+1} - h^{it}) \frac{1}{\theta_s - \theta_r} \right|$$

If $h^{it} \geq h_s \wedge h^{it+1} \geq h_s$

$$\Delta h = \left| h^{it+1} - h^{it} \right|$$

h_s is the pressure near saturation ($\theta_{ef} = 1 - 10^{-15}$). This means that only when the cell is almost saturated HYDRUS will use h differences. Most of the time HYDRUS is really using water content differences to evaluate the convergence of the iterative process. This difference is accessed by multiplying the decline of $\theta(h)$ by an h difference.

4.5-MOHID

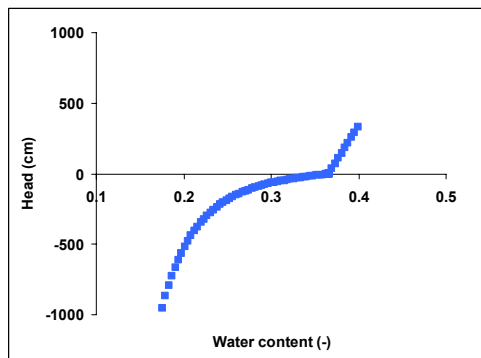
In MOHID, it is the water content variable θ that evolves in time, and h values are evaluated from the retention curve.

$$h(\theta) = - \frac{\left(\theta_{ef}^{-\frac{1}{M}} - 1 \right)^{\frac{1}{N}}}{\alpha}$$

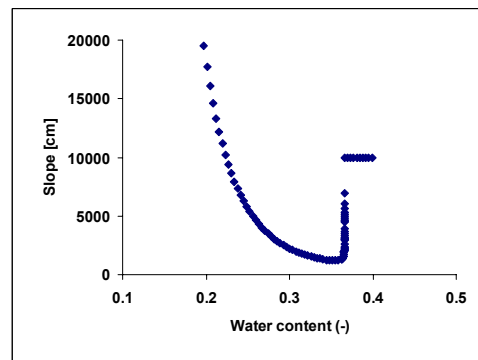
The derivate of this equation corresponds to the inverse of the soil water capacity:

$$h'(\theta) = \frac{1}{\alpha N} \left(\theta_{ef}^{-\frac{1}{M}} - 1 \right)^{\frac{1-N}{N}} * \frac{1}{M} \theta_{ef}^{-\left(\frac{1+M}{M}\right)} * \frac{1}{\theta_s - \theta_r}$$

The next figure shows the shape of this curve and it's derivate.



Water retention curve and the pressure curve for values over the saturation point



Decline for the water retention curve and the pressure curve for values over the saturation point

tetar	tetas	nfit	mfit	alfa	cons	Ss
0.001	0.46	1.142	0.18686	0.02	12.1	1.00E-04

In MOHID, three difference convergence methods are available:

First method:

$$\text{If } h^{it} < 0 \Delta h^{it+1} < 0$$

$$h''(\theta) \min = \min(h''(\theta^{it+1}), h''(\theta^{it}))$$

$$h'(\theta) \max = \max(h'(\theta^{it+1}), h'(\theta^{it}))$$

$$\text{If } h''(\theta) \min > 200$$

$$\Delta h = |\theta^{it} - \theta^{it+1}| * h'(\theta) \max$$

$$\text{If } \Delta h > h_{tol}$$

$$\text{If } h''(\theta) \min \leq 200$$

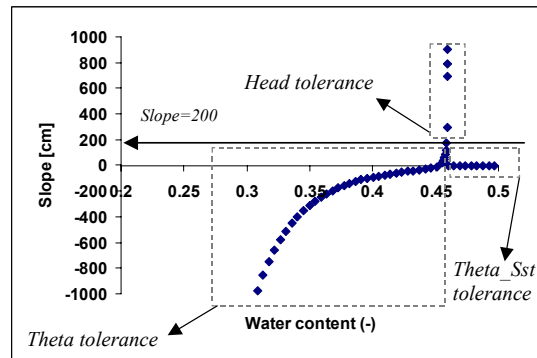
$$\Delta \theta = |\theta^{it} - \theta^{it+1}|$$

$$\text{If } \Delta \theta > \theta_{tol}$$

$$\text{If } h^{it} \geq 0 \Delta h^{it+1} \geq 0$$

$$\Delta \theta = |\theta^{it} - \theta^{it+1}|$$

$$\text{If } \Delta \theta > \theta_{tolSst}$$



Second method:

$$\text{If } h^{it} < 0 \Delta h^{it+1} < 0$$

$$h'(\theta) \min = \min(h'(\theta^{it+1}), h'(\theta^{it}))$$

$$h'(\theta) \max = \max(h'(\theta^{it+1}), h'(\theta^{it}))$$

$$h''(\theta) \min = \min(h''(\theta^{it+1}), h''(\theta^{it}))$$

$$\text{If } h'(\theta) \min > 3000$$

$$\Delta\theta = |\theta^{it} - \theta^{it+1}|$$

$$\text{If } \Delta\theta > \theta_{tol}$$

$$\text{If } h'(\theta) \min \leq 3000$$

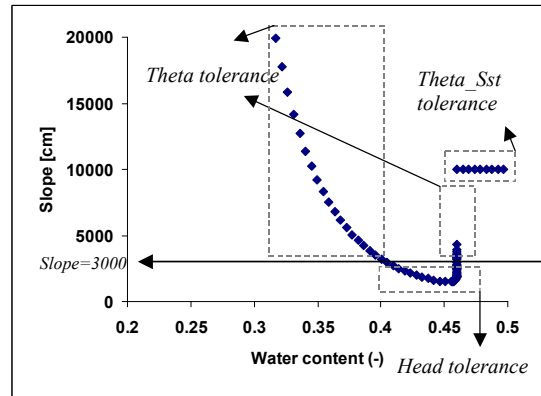
$$\Delta h = |\theta^{it} - \theta^{it+1}| * h'(\theta) \max$$

$$\text{If } \Delta h > h_{tol}$$

$$\text{If } h^{it} \geq 0 \Delta h^{it+1} \geq 0$$

$$\Delta\theta = |\theta^{it} - \theta^{it+1}|$$

$$\text{If } \Delta\theta > \theta_{tolSst}$$



Third type of convergence (<>HYDRUS)

$$\text{If } h^{it} < 0 \Delta h^{it+1} < 0$$

$$\text{If } h^{it} < h_s \Delta h^{it+1} < h_s$$

$$\Delta \theta = \left| \theta^{it} - \theta^{it+1} \right| \text{ where}$$

$$\theta^{it+1} = \theta^{it} + \frac{\partial \theta}{\partial h^{it}} (h^{it+1} - h^{it}) \frac{1}{\theta_s - \theta_r}$$

$$\Delta \theta = \left| \frac{1}{h'(\theta)} (h^{it+1} - h^{it}) \frac{1}{\theta_s - \theta_r} \right|$$

$$\text{If } \Delta \theta > \theta_{tol}$$

$$\text{If } h^{it} \geq h_s \Delta h^{it+1} \geq h_s$$

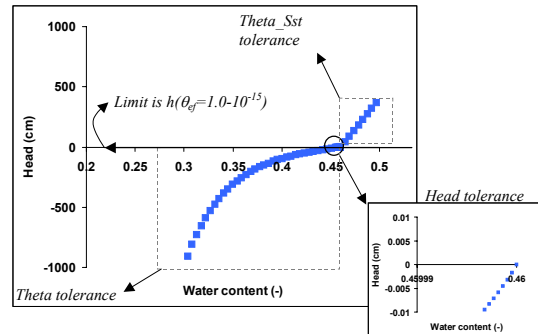
$$\Delta h = \left| h^{it+1} - h^{it} \right|$$

$$\text{If } \Delta h > h_{tol}$$

$$\text{If } h^{it} \geq 0 \Delta h^{it+1} \geq 0$$

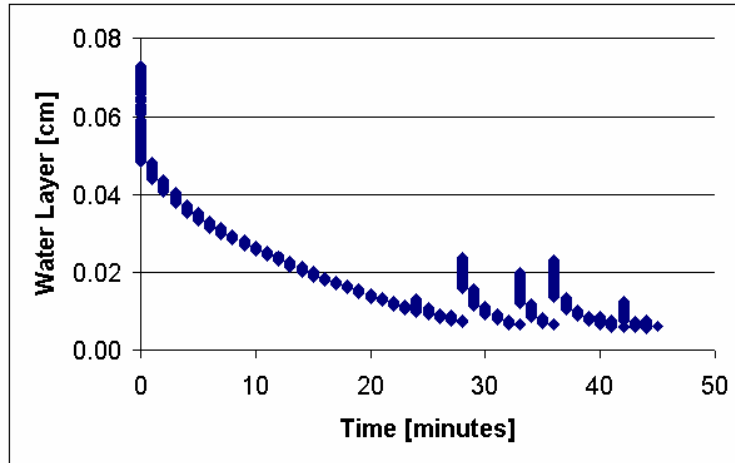
$$\Delta \theta = \left| \theta^{it} - \theta^{it+1} \right|$$

$$\text{If } \Delta \theta > \theta_{tolSst}$$



4.5.1 BEHAVIOR for saturation situations:

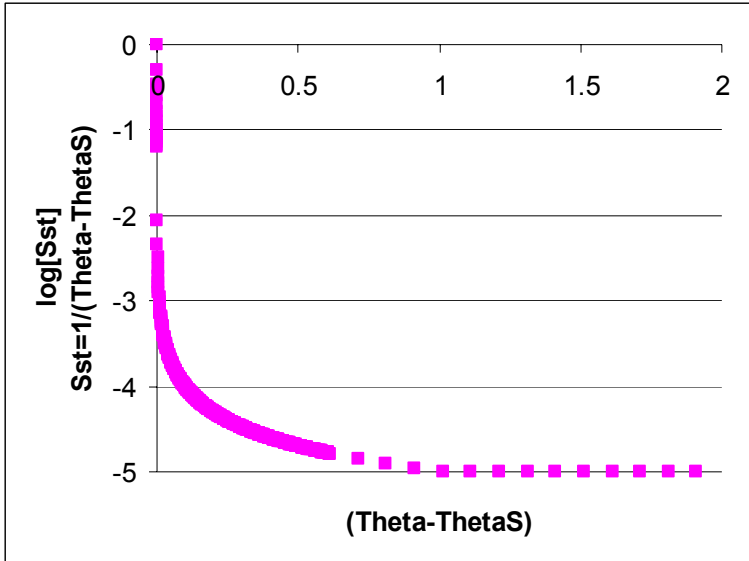
Initially Sst was constant and one of the parameters that needed to be supplied to the mode. However, this approach could lead to instability, has shown in the next figure. In this figure, as more water infiltrated the soil, the higher the pressure terms would become leading to instability. This happened because the selected Sst was too low, and small increases in water content lead to pressure increases. In this case, this variation leads to variant water levels in the surface.



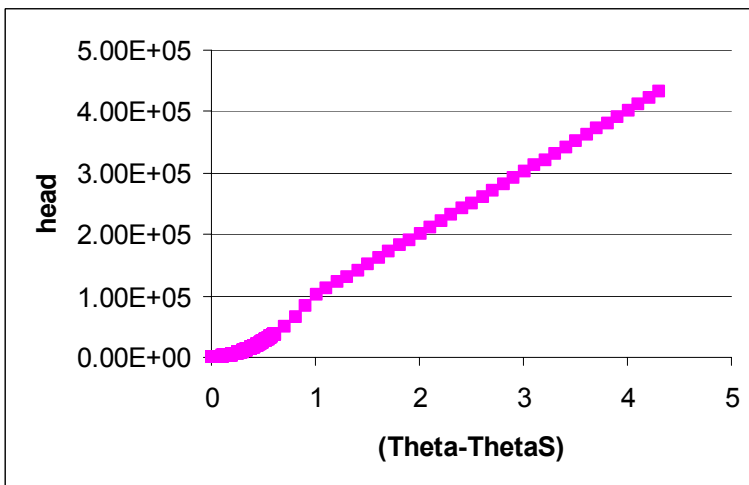
On the other hand, high Sst could lead to water storage in some cells. In order to solve this problem, a SST that varies in function of the water content θ . was implemented. This way, Sst values would be lower for lower values of θ , while for higher values, would be higher. However, in this approach St loses its original definition of specific water storage coefficient

$$Sst = \begin{cases} 1 & se \quad (\theta - \theta_s) = 0 \\ 10^{-4} * \frac{1}{(\theta - \theta_s)} & se \quad 0 < (\theta - \theta_s) \leq 1 \\ 10^{-4} & se \quad (\theta - \theta_s) > 1 \end{cases}$$

The shape of this function is shown in the next plots.



$$h = \begin{cases} 1 * (\theta - \theta_s) & \text{se } (\theta - \theta_s) = 0 \\ 10^4 * (\theta - \theta_s)^2 & \text{se } 0 < (\theta - \theta_s) \leq 1 \\ 10^4 * (\theta - \theta_s) & \text{se } (\theta - \theta_s) > 1 \end{cases}$$



APPENDIX II - Solute transport in unsaturated soil

1- General Overview

Increasing public awareness on significant contamination of ground waters by industrial, municipal and agricultural chemicals has focussed much attention on solute movement in unsaturated soils, creating a burst of experimental and theoretical research in this area (van Genuchten and Jury, as in Jury et al. 1991).

Again, the usual mass conservation statement describes the transport of solute in soils:

Decrease of solute leaving the control volume during $\Delta t =$

- Solute entering soil volume during Δt
- + Solute leaving soil volume during Δt
- + Solute sinks
- Solute sources

The mass of solute present in the soil is represented by:

$$Vol_w * C_w \quad (1)$$

Considering a water transport flux \vec{J}_{WT} , the volume of solute entering the soil is evaluated by:

$$\vec{J}_{WT} * C_w \cdot \vec{n} ds \quad (2)$$

This is a flow per unit area of "total soil", so in order to obtain the total solute mass entering the control volume one has to integrate (2) over the control surface.

On the other hand the water volume contained in an elemental volume dV of soil is:

$$\iiint_v \theta dV \quad (3)$$

Considering that θ is the volumetric water content.

Combining (3) and (1), the time rate of increase of mass inside the volume V for an infinitesimal Δt is then:

$$\frac{\partial}{\partial t} \iiint_v \theta C_w dV \quad (4)$$

In turn the time rate of decrease is

$$-\frac{\partial}{\partial t} \iiint_v \theta C_w dV \quad (5)$$

Combining Error! Reference source not found., (5) and (4):

$$\frac{\partial}{\partial t} \iiint_V \theta C_l dV = - \iint_S J_{WT} C_w \cdot \vec{n} ds \quad (6)$$

Since the control volume used in the derivation of (5) is fixed in space, it doesn't change in time, and hence the time derivative $\partial/\partial t$ can be placed inside the integral.

$$\iiint_V \frac{\partial}{\partial t} \theta dV \quad (7)$$

Using the divergence theorem the right hand side of (5) becomes:

$$\iint_S \vec{J}_{WT} C_w \cdot \vec{n} ds = \iiint_V \nabla \cdot \vec{J}_{WT} C_w dV \quad (8)$$

Using (6), Error! Reference source not found. in (5) we have:

$$\iiint_V \left[\frac{\partial \theta C_w}{\partial t} + \nabla \cdot \vec{J}_{WT} C_w \right] dV = 0 \quad (9)$$

or:

$$\frac{\partial \theta C_w}{\partial t} = -\nabla \cdot \vec{J}_{WT} C_w + r_w \quad (10)$$

Equation (5) is the integral form of the water conservation equation while (10) is the partial differential equation of the continuity equation. Equation (10) could have been obtained directly from the mass balance of an infinitesimal small element fixed in space. Never less, both of them are in the conservative form.

In MOHID, the integral form of the transport equation is solved using the ADI method for temporal discretization,. Note that (6) for incompressible soil is equivalent to:

$$\frac{\partial Vol_{water} C_l}{\partial t} = \iint_S \vec{J}_{WT} \cdot \vec{n} ds \quad (11)$$

For more information on ADI and the way, MOHID discretizes the transport equation can be found in Leitão 2002.

2- Solute Flux in soil

In the previous chapter a solute flux termed $\vec{J}_w * C_w$, was presented without further considerations.

This flux is considered to be the sum of two terms, the bulk transport flux and the diffusive flux. The bulk flux is formally written has:

$$\vec{J}_w C_w$$

However \vec{J}_w is an approximate quantity that has been averaged over many soil pores and does not represent actual water flow path that must curve around soil particles and air spaces.

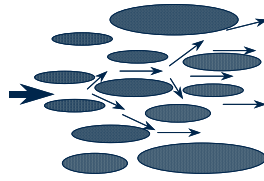


Figure 2.1- Dispersive effect

In soil, this erratic transport by hydrodynamic dispersion has been studied over the years. A special case of all possible flows, the convective – dispersive transport (Jury et al. 1991), occurs in porous media under the following two conditions:

If these conditions are satisfied, the hydrodynamic dispersive flux is identical to the diffusion flux (Bear, 1972)

$$J_{th} = -D_{th} \frac{\partial C_l}{\partial z}$$

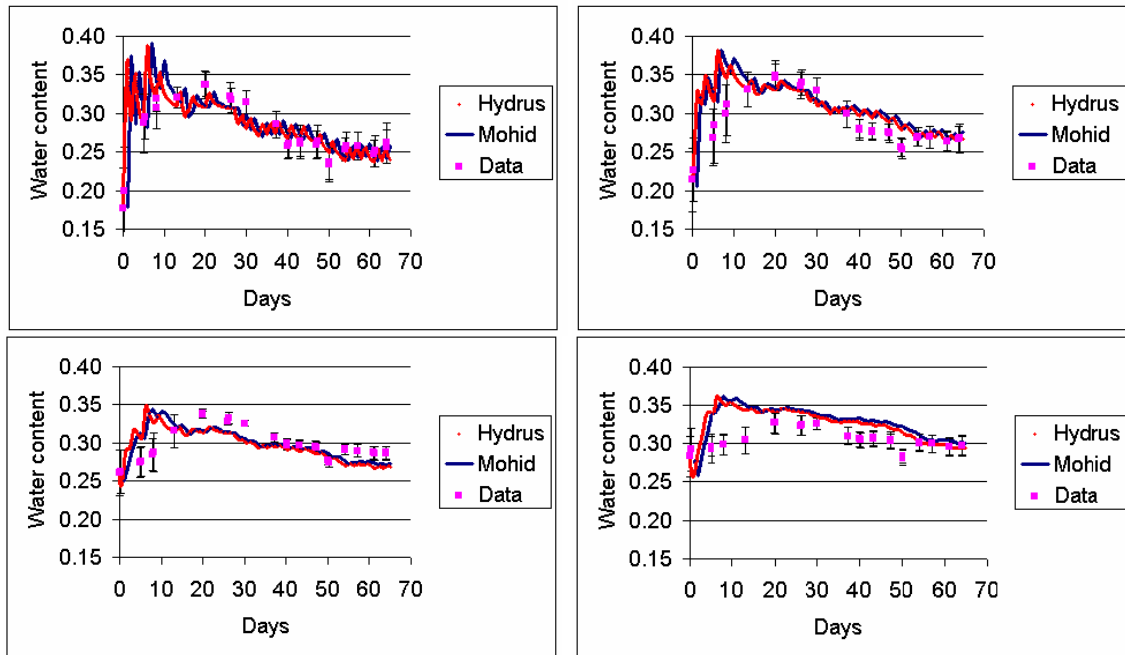
where D_{th} (in centimetres squared per day) is the hydrodynamic dispersion coefficient. This coefficient is considered proportional to the pore water velocity $v = \bar{J}_w / \theta$ (Bear 1972).

$$D_w = \lambda v$$

Where λ in centimetres per day is the “dispersivity”. Typical values of λ are 0.5-2 cm in packed laboratory columns and 5-20 cm in the field. (Jury et al. 1991). Adding to this “turbulent” flux the molecular diffusivity coefficient can be added. However, the hydrodynamic diffusive flux is usually the dominant effect.

APPENDIX III - Alvalade Data

The next figures illustrates the comparison between MOHID and HYDRUS for soil water flow in Alvalade. The same data was later used to evaluate sodium transport see Chambel- Leitão 2002.



Measured Hydraulic properties of the soil.

<i>Depth</i>	θ_R	θ_S	<i>alfa</i>	<i>n</i>	<i>ks</i>	<i>L</i>
0-48	0	0.4270	0.0292	1.208	18.24	-4.391
48-85	0	0.4275	0.1083	1.161	99.30	-5.909
85-100	0	0.3727	0.0395	1.154	21.36	-6.913

APPENDIX IV –Macro Programing

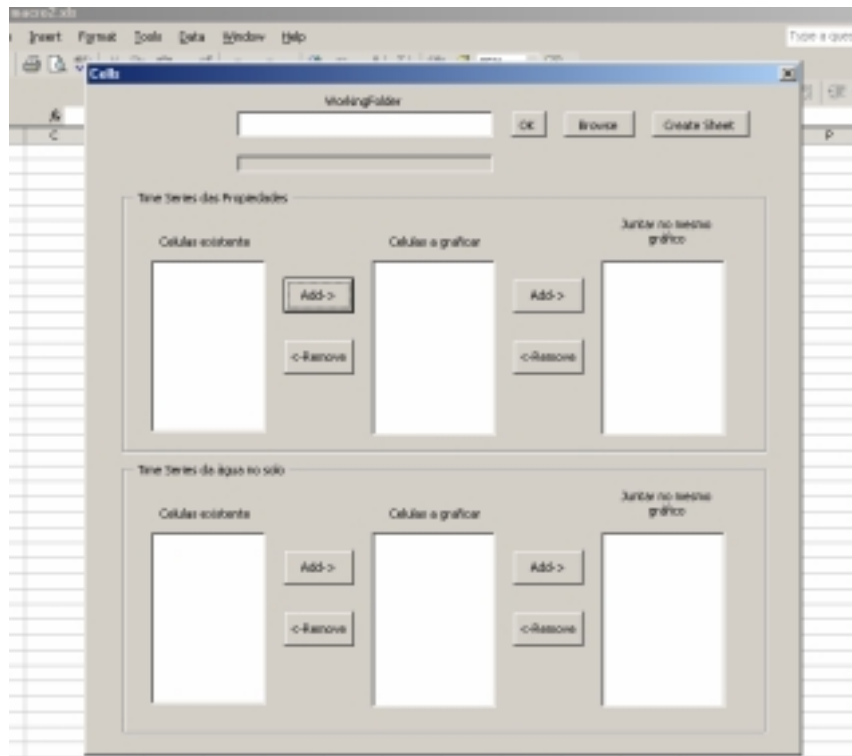
Output treatment using The VBA language applied to Microsoft EXCEL

Processing massive amounts of data, dispersed trough various ASCII files of time series, can be an arduous task.

VBA macros where developed to create the graphic presented in this work.

The developed program, allows the user to select which time series he desires to process, saving time in data processing.

A second macro as also developed during the FORTRAN code-implementing period to compare FORTRAN and POWERSIM results.



APPENDIX V- Brief MOHID history

MOHID

This document describes the soil water modelling modules of the three-dimensional water modelling system Mohid.

Actually the principal investigators are Ramiro Neves, Paulo Chambel Leitão and Frank Braunschweig, from the Technical University of Lisbon. Contributions from Henrique Coelho, Manuel Villarreal (Turbulence) and Pedro Pina (Water Quality) are also included in the model. A lot of other investigators have given their contribution to this model over the past years.

History

The development of the *Mohid* model started back in 1985, passing since this time through continuously updates and improvements due to its use during different projects of scientific research and engineering projects. Initially the *Mohid* water modeling system was a bi-dimensional hydrodynamic model, called *Mohid 2D* (Neves, 1985). This model was used to study estuaries and coastal areas using a classical finite difference approach. In the following years, a bi-dimensional eulerian and lagrangian transport model were included in this model. The first three-dimensional was introduced by Santos (1995), which used a vertical double Sigma coordinate. This version was called *Mohid 3D*. The limitations of the double Sigma coordinate revealed the necessity to develop a model which could use a generic vertical coordinate, permitting the user to choose the type of vertical coordinate, depending on the study area. Due to this necessity the concept of finite volumes was introduced with the version *Mesh 3D* by Martins (1999). In the *Mesh 3D* model were included a three dimensional eulerian transport model, a three dimensional lagrangian transport model (Leitão, 1996) and the zero-dimensional water quality model (Miranda, 1999). Since the introduction of the finite volumes approach, this discretization remains in the model *Mohid*.

Actual State

With the growing model complexity, it was necessary to introduce a new way in the organization of the information of the *Mohid* model. In 1998 the whole code was submitted to a complete rearrangement, using new the feature of programming languages and also the capacities of the computer to reprogram the whole *Mohid* model. The main goal of this rearrangement was to turn the model more robust, reliable and protect its structure against involuntary programming errors, so it would be more easily "grow able". To achieve this goal, objected oriented programming in FORTRAN was introduced to the *Mohid* model, like described in Decyk (Decyk, *et al.*, 1997).

The philosophy of the new *Mohid* model (Miranda, *et al.*, 2000), further on simple designated *Mohid*, permits to use the model in any dimension (one-dimensional, two-dimensional or three-dimensional). The whole model is programmed in ANSI FORTRAN 95, using the objected orientated philosophy. The

subdivision of the program into modules, like the information flux between these modules was object of a study by the *Mohid* authors.

Actually the model *Mohid* is composed by over 40 modules, which complete over 150 mil code lines. Each module is responsible to manage a certain kind of information.